A realistic US Long-haul Drive Cycle for Vehicle Simulations, Costing and Emissions Analysis

A realistic US Long-haul Drive Cycle for Vehicle Simulations, Costing and Emissions Analysis

Rob Jones[‡a], Moritz Köllner[‡a], Kariana Moreno-Sader[a], Dávid Kovács[b], Thaddaeus Delebinski[b], Reza Rezaei[b], William H. Green[*a]

[a] *Department of Chemical Engineering, Massachusetts Institute of Technology, Cambridge, Massachusetts 02139, United States*

[b] *IAV GmbH, Nordhoffstr. 5, Gifhorn 38518, Germany*

Abstract

While heavy-duty trucks constitute the backbone of freight transportation in the US, they also contribute significantly to greenhouse gas emissions. Various alternative powertrains to reduce emissions have been assessed, but few specific to US long-haul applications with a consistent basis of assumptions. To enable a more accurate assessment for all stakeholders, a representative drive cycle for long-haul truck operations in the US is introduced (USLHC8) for modeling and simulation purposes. It was generated from 58,000 miles of real-driving data through a unique random microtrip selection algorithm. USLHC8 covers a total driving time of 10 h 47 min, an average vehicle speed of 55.58 mph, and road grade ranging from -6% to +6%. To establish a benchmark for further powertrain comparisons, a vehicle-level simulation of a conventional diesel powertrain was paired with USLHC8. Benchmarks are presented for fuel consumption, Well-to-Wheel emissions and Total Cost to Society under different scenarios (present-day, mid-term and long-term).

Keywords: Long-haul, Drive cycle, Diesel, Powertrain, Emissions

[‡]These authors contributed equally, * Corresponding author: whgreen@mit.edu

1 Introduction

Slowing climate change is a major challenge for the world. Reducing carbon dioxide emissions is particularly difficult in the long-distance transportation sector, particularly for heavy-duty trucking [1]. Heavy-duty freight trucks are responsible for approximately 30% of US highway transportation emissions, even though they only represent about 5.5 % of vehicles on the road [2]. Heavy-duty trucks are also the backbone of the US economy, as they account for 71 % of freight deliveries [3]. The corresponding on-road freight energy consumption has been consistently increasing over the last decades and is expected to grow even further in the future [4, 5].

The fast growth of heavy transport, which relies heavily on diesel engines, has motivated regulations intended to reduce CO_2 emissions. For instance, the United States Environmental Protection Agency (EPA) mandates a CO_2-reduction of 27% in 2027 relative to a 2017 baseline for commercial trucks [6].

In Europe, the proposal from the Consortium for ultra Low Vehicle Emissions (CLOVE) strengthening NO_x limits for the Euro VII heavy-duty vehicle legislation. These efforts in lowering emissions have also uncovered challenges in the context of heavy-duty engine developments. Different alternative powertrains are being explored to answer the crucial question: how can road freight emissions be cut dramatically by 2050 while at the same time facing a growing transportation demand? The complexity of this question presents a challenging dilemma for the transportation sector: neither the scientific community nor large truck manufacturers have reached a consensus on which powertrain will be the best solution for the future of the long-haul sector. This lack of consensus slows decision-making among stakeholders. For example, policymakers are hesitant on large-scale incentives, and private-sector investors avoid substantial uncertainty. Uncertainty about which fuel/powertrain combination will dominate in the future makes it even more expensive and risky for manufacturers to carry the burden of research and development costs for a multitude of different possible future powertrain solutions. Lastly, truck operators are uncertain which powertrains to purchase for their fleet to comply with future regulations and customer sustainability demands. Comparative analyses of alternative powertrains have been performed to clarify the path to decarbonize long-haul trucks [7, 8, 9], primarily from economic and environmental criteria. While these comparisons have provided insights into the trade-offs of switching from diesel-based to cleaner technologies, comprehensive assessments with a focus on long-haul trucking operations are still limited, particularly for the US freight operation, where driving patterns are different than in other countries. This makes it more difficult to evaluate technologies on a consistent basis when it comes to different vehicle models, design attributes, and assumptions about how the trucks will be employed [10]. A representative long-haul class 8 drive cycle is an essential prerequisite to accurately compare suitable alternative powertrains on a consistent basis. In general terms, a drive cycle consists of a series of data points that describe a vehicle speed trace over time. Drive cycles are the main input for most simulations determining on-road energy consumption and emissions. Also, drive cycles influence the sizing and performance requirements of the powertrain components. The purpose of this study is twofold:

1. Develop a characterization of US long-haul freight operations in the form of a drive cycle and associated supplementary parameters.
2. Using the results from 1, establish a benchmark to conventional long-haul trucking on the basis of fuel consumption, greenhouse gas (GHG) emissions, and total cost to society (TCS), for comparison with alternative powertrains in the present, mid term, and long term.

In the future, this new drive cycle can be used to assess proposed fuel/powertrain combinations and compare them with the "conventional diesel" benchmark presented here. This paper is organized as follows. Section 2 provides a literature review on drive cycles currently used to model long-haul truck operation. This section also gives background on comparative analyses of different powertrains and current research gaps. Section 3 outlines the methodology followed for the drive-cycle construction, vehicle-level simulation, emissions analysis and Total Cost of Ownership (TCO) analysis. Results are presented in section 4. The paper concludes with section 5, outlining final remarks, limitations and future directions.

2 Literature Review

In the reviewed literature on heavy-duty truck emissions modeling in the USA, six commonly used drive cycles were identified for long-haul trucking. Namely:

1. Highway fuel consumption Driving Schedule (HWFET) [11]
2. Heavy-Duty Diesel Truck Cruise Mode (HHDDT) [12]
3. Northeast States Center for a Clean Air Future Long-Haul Cycle (NESCCAF) [13]
4. US06 Supplemental Federal Test Procedure [11]
5. Heavy-Duty Urban Dynamometer Driving Schedule (HDUDDS) [11]
6. NREL long-haul cycle [14]

These six driving cycles are shown in Figure S1. These are used for simulating highway duty cycles, and most are intended for chassis dynamometer testing. However, they have significant shortcomings in terms of simulating entire long-haul duty cycles on the basis of distance traveled, duration, vehicle speed and road grade distributions, and driving behavior.

The distance and duration of a drive cycle can determine the size and weight of the energy storage on board a truck that is necessary to cover a given route. Energy storage sizing considerations are especially important for alternative powertrains such as battery and fuel cell electric trucks that suffer from low energy density. The distance and duration can be increased by repeating a given drive cycle several times. However, if the initial drive cycle does not accurately represent the power requirements of the entire duty cycle or does not contain uninterrupted highway driving segments that are long enough to represent long-haul driving, a repetition of the drive cycle leads to an inflated frequency of vehicle stops and less realistic power demand distribution.

Except for the NREL long-haul cycle, all cycles reviewed are too short in distance and duration to represent long-haul driving. They range from 6 to 103 miles, and from 10 to 114 minutes. The NREL long-haul cycle on the other hand is too long, consisting of 935 miles traveled in more than 19 hours. This length and duration would only be appropriate for slip seating operations, in which multiple drivers successively operate a single truck. For the overall long-haul sector, slip seating operation has a limited significance because it requires very complex and costly logistics for allocating drivers given the current shortage of truck drivers in the US [15, 16] (Slip-seating is more important at shorter distances for return-to-base operations).

A drive cycle's vehicle speed and road grade distributions are directly related to a vehicle's tractive power demand and, consequently, to the fuel consumption and powertrain component sizing. The HWFET, HDUDDS and HHDDT are limited to vehicle speeds ranging up to 60 mph and thus lack the higher speeds driven in many states. This leads to an under-representation of the national average power demand. The NESCCAF is a modified version of the HHDDT that is designed to have higher vehicle speeds and longer driving time. However, the additional driving time is generated by adding modal segments that do not contain the transients that are representative of real driving. Therefore, the NESCCAF modal segments underestimate power demand due to the absence of accelerations. Of the six drive cycles discussed, only the NREL long-haul and NESCCAF cycle account for road grade. Even if the total elevation changes for a given driving profile were to be negligible over time, information about the road grade would still be of great importance to determine the instantaneous power demand which defines the performance requirements for the powertrain sizing. While the NESCCAF cycle contains a road grade profile, it is synthetically contrived to oscillate between -3% and 3% road grade and does not represent a realistic road grade profile. The NREL long-haul cycle represents a particular continuous driving event and thus only accounts for a single set of vehicle, driver and route characteristics. This significantly limits its representativeness to the aggregate national average long-haul driving profile. Since no representative US long-haul driving cycle has been published, light-duty drive cycles including the HWFET and US06 are sometimes used for highway driving. This leads to a significantly higher power demand because of the increased number and speed of acceleration events for light-duty vehicles compared to long-haul heavy trucks. Hence, a more realistic drive cycle for long-haul driving is needed to accurately determine road freight emissions for long-haul class 8 trucks. This need was also expressed by the US EPA in its report on GHG Certification of Medium- and Heavy-Duty Vehicles [17].

Studies on powertrain simulation, emissions analysis and TCO are widely available in the literature. For example, Lee et al. [18] conducted a well-to-wheel (WTW) analysis of the emissions for conventional diesel and hydrogen fuel cell electric trucks (FCET) over a range of Class 2b through Class 8b trucks. They derived the truck fuel consumption from vehicle dynamic simulation using the Autonomie model and an adjusted version of EPA/NHTSA test cycles. Langshaw et al.[19] also compared two different fuel options, diesel and LNG, in the context of food freight with a large UK Food Retailer as a case study. They estimated the GHG emissions, Total Cost of Ownership (TCO) and Total Cost to Society (TCS) using real data of duty cycles that were recorded by the food retail company. This data corresponded to measurements in fuel consumption and distance traveled for diesel and LNG vehicle fleets, which was then translated into vehicle energy efficiencies. Recently, Lajevardi et al.[9] analyzed several options for conventional and alternative short-haul and long-haul drivetrains over different scenarios of infrastructure deployment. When it comes to fuel consumption, they used in-house models for these drivetrains with drive cycles that represent freight operations in British Columbia.

The literature review on powertrain emissions and TCO revealed several research gaps. First, few studies compare powertrain performance in the mid and long term. This is particularly relevant because technology adoption and maturity could overcome the current limitations of alternative long-haul powertrains, leading to more competitive options vs. the conventional diesel powertrain in the future. Second, various works focus on different geographical regions, such as British Columbia [9], which may differ significantly from the average US long-haul trucking sector. Third, few works provide a consistent basis of assumptions, which is necessary for a comprehensive comparison of alternative powertrain options for long-haul trucks [18].

3 Methods

3.1 Defining Long Haul

3.1.1. Regional Haul vs. Long Haul

In the context of freight operations, the duty cycles of most class 8 trucks can be classified into regional-haul and long-haul. This work focuses on long-haul operation because it is significantly more complex to equip with alternative powertrains due to the need for prolonged high-power output over extended highway distances. In addition, regional return-to-base operation enables for better maintenance and simpler overnight vehicle charging or refueling at the home base [20].

Several different criteria for distinguishing "long-haul" from other trucking have been proposed in the literature. Here, long-haul operation is distinguished from regional-haul on the basis of trip distance and average vehicle speed. Table 1 lists different values for long-haul driving distances and speeds proposed in the literature. In this paper, class 8 long-haul truck operation is defined as trip distances of at least 250 mi with a minimum average vehicle speed of at least 40 mph.

This minimum distance of 250 miles was determined based on the average of the reviewed literature as shown in Table 1 and currently available alternative powertrains. At the time of completion of this work, one of the leading commercially available class 8 trucks with an alternative powertrain had a 250-mile all electric range [21]. The minimum average vehicle speed that long-haul trucks reach during a day trip was determined to be 40 mph because line haul trucks in California, the state with the most conservative truck speed limit [22], were ascertained to have an average vehicle speed of 41.1 mph with mostly highway driving [23].

3.1.2. Long-haul Fraction of Class 8 Market

Data on the US. truck population from the most recent Vehicle Inventory and Use Survey (VIUS) was employed to determine the fraction of class 8 trucks being used for long-haul operations. Two different approaches were considered. The first approach distinguished the tractors with sleeper cabs as long-haul, since they allow operation without returning to a home base or depot. According to this approach, the long-haul fraction of the class 8 market was 26.8% (see Figure S2). The second approach distinguishes long-haul based on a daily driving range greater than 250 miles per day. For this approach, the VIUS data in miles per year was translated into daily miles using the number of months operated, 30.4 days per month conversion factor.

Based on the output space of these daily ranges, depicted Figure S3, the long-haul fraction was 24%. Both approaches were combined, defining the long-haul fraction of the class 8 market at 25%.

3.1.3. Vehicle Lifetime

This work considers the entire useful vehicle life of an average class 8 tractor. After their first use in long-haul operations, long-haul tractors typically have a second-use phase, where they travel shorter distances as shown in Table S1. The latter applications have lower requirements in terms of engine performance and uptime in between service intervals because of their shorter distances and driving durations. The repurposing of trucks is an established market process that is financially incentivized and will very likely continue to take place in the future. Consequently, the long-haul use-phase should not be analyzed in isolation from secondary use when regarding emissions. In the reviewed literature, there are very consistent assumptions establishing the length of the vehicle lifetime at 10 years (see Table 1). In this work, the vehicle lifetime was therefore defined as 10 years. This longer lifetime assumption instead of a first-use period enabled better comparison of alternative powertrains in terms of in-use emissions, replacement, and durability. However, it is important to keep in mind that the way the truck is used during its "secondary use" years will be significantly different from the "first use" phase of its life, but still operating as "long-haul".

3.1.4. Vehicle Miles Traveled (VMT)

The VMT parameter was defined per year of operation within the entire vehicle life of 10 years to represent both first-use and second-use operation characteristics. These values derived from the VIUS dataset for class

Table 1: Parameters defining long-haul operation

Parameters	Values	Units	Reference
Minimum daily trip distance	>300	mi	NACFE [24]
	190	mi	[25]
	220-250	mi	[26]
	250	mi	This work
Minimum average vehicle speed in a daily trip	41.1	mph	[23]
	40	mph	This work
Vehicle lifetime	10	years	[27, 28, 29], this work
	5	years	[30]
	3	years	[31]
Vehicle miles traveled	120,000	mi/year	[30]
	1,500,000	mi/lifetime	[7]
	1,000,000	mi/lifetime	[32]
	104,000	mi/year	[33]
	91,506	mi/year	[34]
	52,000-108,000	mi/year	[27, 35], this work
Maximum driving hours	11	hours	[36]
Daily range	750	mi/day	[37, 38]
	600	mi/day	[24]
	587	mi/day	(J. Gregorio, personal communication, September 5, 2021)
	600	mi/day	This work

8 sleeper cabs [27] and are available in Table S1. The average VMT per year over the vehicle life is 87,200 miles and the cumulative VMT after ten years is 872,000 miles [27, 35].

3.1.5. Daily Range

With respect to the legal limits for truck operation, a drive cycle length of 600 miles was chosen, which is also consistent with estimations of NACFE and other works summarized in Table 1. This value is also supported by the VIUS daily range for sleeper cab class 8 trucks distribution given in Figure S4.

3.1.6. Vehicle Weight

The vehicle weight has a substantial influence on fuel consumption and thus on emissions and operating costs. The average vehicle curb weight of a standard diesel heavy-duty sleeper tractor was defined as 19,500 lb based on averaging data from [39] and adding the average weight of a full tank of diesel fuel [40]. The defined weight is consistent with standard heavy-duty sleeper tractors such as the 2011 Freightliner Cascadia 133 [41]. To enable further research regarding alternative powertrains, the glider weight was also determined at 14,991 lb, defining the weight of the tractor without the powertrain. This was done by subtracting the weight of all components specific to a diesel powertrain from the defined tractor curb weight. The derived glider weight is consistent with [42]. The average tractor payload for class 8b trucks was taken to be 40,600 lb accounting for both trailer and cargo weight. It was derived using a filtered subset of the most recent

dataset from the SmartWay program [43]. The combined average tractor and payload weight is consistent with Zhao et al.[44].

3.2 Drive Cycle Development

The drive cycle presented in this paper consists of a vehicle speed and a road grade trace. It was developed by first determining the characteristics of the national average driving profile of long-haul class 8 trucks and then generating a drive cycle from real driving data, taken from the NACFE Run On Less Regional (ROLR), that best describes these characteristics. The matching was done by optimizing selected assessment features relative to a target feature vector. Figure 1 shows a schematic representation of the steps followed for the drive cycle construction. Brief descriptions of each step are provided below. More details are available in the supplementary material.

3.2.1. Assessment Feature Selection

In the context of this paper, an assessment feature describes one or several driving characteristics and is used to quantify the national average driving profile. Out of 10 identified assessment features, the 3 features vehicle speed, road grade, and daily range were chosen to quantify the national average driving profile as they have the largest impact on powertrain energy demand. The powertrain energy demand is a suitable metric since it is strictly proportional to fuel consumption and thus $CO_2eq - emissions$.The impact of assessment features on the energy demand was determined by (i) evaluating their relative impact on each vehicle tractive force component and (ii) combining this with an analysis that calculated the relative impact of each tractive force component specific to long-haul truck driving [45].

3.2.2. Target Feature Vector Definition

The target feature vector describes the national average values of long-haul truck driving for the chosen assessment features of vehicle speed, road grade, and daily range. This vector was used to optimize the drive cycle generation by minimizing the deviation between a generated drive cycle's feature vector and the target feature vector. Based on public availability of high-resolution data specific to heavy-duty trucks, this vector was constructed from the following datasets:

1. NACFE Run On Less 2017 Roadshow (ROL17) [24]
2. NACFE Run On Less Regional Roadshow (ROLR) [46]
3. US Bureau of Transportation Statistics (BTS) Freight Analysis Framework [47]
4. Oak Ridge National Laboratory Heavy Truck Duty Cycle Project (HTDC)
5. NREL Fleet DNA [48]
6. TomTom N.V. National Road Grade database [49]

A summary of the characteristics of each dataset is given in Table S2.

To increase the representativeness on a national level, the vehicle speed part of the target feature vector was constructed from several vehicle speed datasets covering a wide variety of characteristics. In order to combine several datasets into one national average vehicle speed distribution, the contribution of each single dataset, i.e. the individual share in the combined national average, had to be determined. The following factors were used to determine the individual contribution of each dataset to the target vector:

- Number of trucks (indicates coverage of different vehicles, routes, and driver behaviors)
- Total mileage covered (indicates coverage of different truck speed limits and traffic characteristics)
- Time duration of data collection (indicates coverage of temporal variations such as changing seasons)
- Geographical coverage (with a focus on major freight corridors)
- Focus on long-haul driving (driving characteristics and stated goal of the data collection effort)

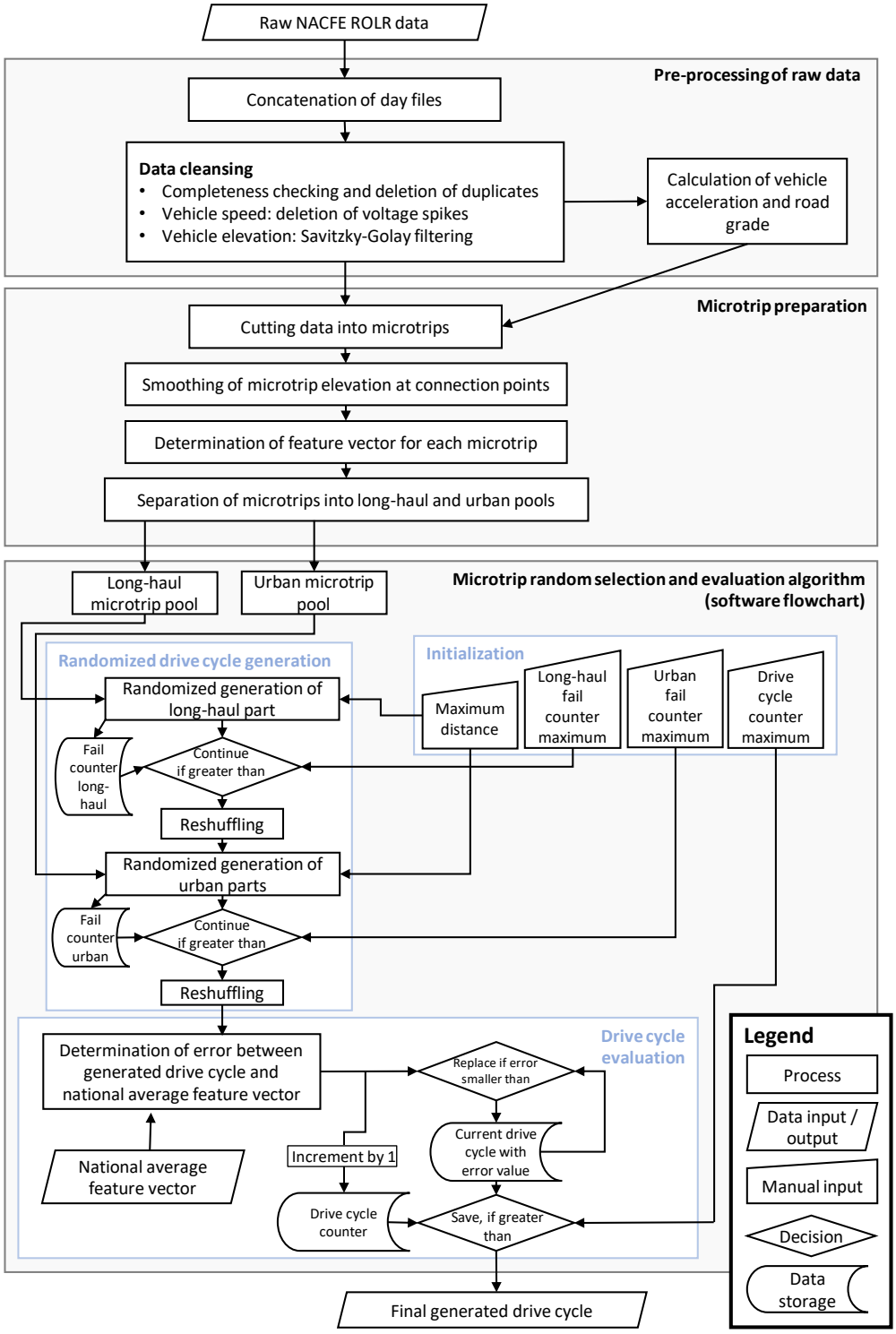

Figure 1: Flowchart of drive cycle generation process

Based on these factors and using the national distribution of truck highway speed limits derived from [17] as a reference, a combination of the datasets with the following individual shares was chosen: 70% HTDC, 20% ROL17, 5% ROLR and 5% filtered Fleet DNA. HTDC was chosen as the primary contributor, as it was the largest dataset available (accounting for almost six times the mileage of all other datasets combined, with comprehensive geographical coverage). The combination of these four datasets represents the target national average vehicle speed, which the generated drive cycle was modeled to match. The defined national average vehicle speed distribution together with different dataset combinations is displayed in Figure S5.

The road grade part of the target feature vector was based on a comprehensive effort by NREL, EPA, and DOE to compile a national representative road grade distribution specifically for medium and heavy-duty trucks using the TomTom N.V. National Road Grade database[17]. The feature vector was constructed from five activity-weighted, distance-based cumulative distributions of absolute road grade [49], each of which is specific to one highway truck speed limit (shown in Figure S6). These 5 truck speed specific distributions were combined into a single distribution independent of the speed limit by multiplying each distribution with the corresponding highway truck speed limit share.

To obtain the final target road grade vector, the single distribution was divided into negative and positive road grade intervals. This was done to ensure a uniform distribution of highway stretches with a positive road grade and a negative road grade in the final drive cycle.

The resulting target vector for vehicle speed and road grade is given in Table S3.

3.2.3. Drive Cycle Generation

The presented drive cycle was generated from real driving data to account for the transient nature of truck driving and thus to estimate its energy demand more accurately than synthetic drive cycles often used in the literature [13, 50]. The NACFE ROLR was selected as the real driving base dataset because of its high-resolution data at 1 Hz for a simultaneously recorded set of vehicle speed and road grade, specific to heavy-duty trucks [24]. It is important to note that both traces were recorded simultaneously to accurately capture the interdependence between vehicle speed and road grade, avoiding unrealistic power requirements. Even though the ROLR dataset as a whole may not fully represent long-haul driving, the drive cycle is generated from subsets of the dataset exhibiting long-haul driving characteristics.

As shown in Figure 1, the drive cycle generation process has three major steps: pre-processing of raw data, microtrip preparation and, microtrip random selection and drive cycle evaluation. More detailed explanations are given in the supplementary material. The pre-processing of the raw ROLR vehicle speed and elevation traces covered data cleansing to remove unrealistic, incomplete and duplicate datapoints. In particular, the GPS-derived elevation data had to be denoised using the Savitzky-Golay filter to be able to decrease the unrealistic volatility in the derived road grade trace.

The second step- microtrip preparation- divides the ROLR data into microtrips by cutting the traces in between periods of driving when the truck is at a complete stop (vehicle speed and acceleration equal zero). The elevation signal at these connection points was smoothed to ensure that the resulting road grades were also always equal to zero. In this way, microtrips can be randomly connected to each other without inconsistencies at the connection points. For each microtrip, the feature vector was calculated containing the total distance driven, and the road grade and vehicle speed distributions. Finally, the microtrips were classified into long-haul and urban using the criteria in Table S4 for the random selection algorithm.

For the microtrip random selection and evaluation step, an algorithm was developed that consists of three main processes, framed in light blue boxes in Figure 1. Namely, these main processes are initialization, randomized drive cycle generation and drive cycle evaluation. In the initialization, manual inputs determining the iterations of the algorithm and the length of the drive cycle are defined. The randomized drive cycle generation process constructs a drive cycle by first concatenating random long-haul microtrips to a long-haul segment. Then, urban microtrips are randomly added to either end of the long-haul segment. This was done to ensure a succession of microtrips that is representative of long-haul driving.

Finally, the feature vector of each generated drive cycle is evaluated against the defined target feature vector of the national average driving profile. The drive cycle with the smallest error value was selected and named US Long-Haul Class 8 drive cycle or USLHC8.

The validation of the USLHC8 was performed using a two-sample Kolmogorov-Smirnov (KS) test against the drive cycles commonly used in the literature. This was done to determine the degree of similarity and thus the representativeness relative to the defined national average driving profile for each drive cycle. In

addition, the robustness of the drive cycle generation methodology itself was evaluated. A drive cycle named "Control" was generated with a slightly altered algorithm for that purpose.

3.3 Diesel heavy-duty Truck Model

A diesel heavy-duty truck (DICET) model was constructed using the software GT-Suite to serve as a baseline to compare alternative powertrains in future research. The developed drive cycle USLHC8 is the main input for DICET model simulations. The tractive power demand is calculated from the drive cycle's vehicle speed and road grade discussed above, and that power demand is met by the powertrain. The output of the model is fuel consumption, which is also used to calculate GHG emissions.

3.3.1. Description of Diesel Truck Model Components

An overview of the DICET model is given in Figure 2. The main model components are the vehicle body, wheels, trailer, engine, engine control unit, transmission, and transmission control unit. The driveline is contained within the vehicle and trailer blocks. The base template for a conventional truck was obtained from the GT-DRIVE+ package and its components were adapted to suit the objectives of the research project. A brief description of each component modeled is given below.

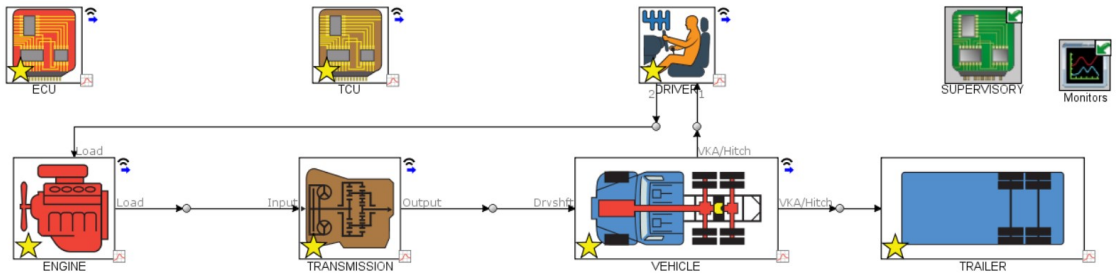

Figure 2: Diesel model overview

The heavy-duty (HD) diesel engine was modeled using an engine map based approach. Thus, no detailed, predictive simulation of the air path, the combustion process, or NO_x emissions is carried out. Instead, steady-state engine maps are used to describe e.g. the engine performance, friction and fuel consumption characteristics. The baseline engine map used for the model represents a contemporary HD diesel engine. The engine maps were obtained through collaboration with IAV GmbH. The selected, 12 L class HD diesel engine features charge air cooled turbocharging, high pressure EGR, and has 2600 Nm of peak torque and a rated power of 370 kW. An overview of the engine properties is presented in Table 2.

Table 2: Specification of selected HD Diesel engine

Engine feature	**Value**
Displacement	12 L class
Number of cylinders	6
Number of valves	4 per cylinder
Compression ratio	18.5:1
Injection system	Direct injection, common rail
Charging system	Turbocharged, charge air cooled
Exhaust gas recirculation (EGR)	Cooled, high pressure EGR
Maximum brake torque	2600 Nm between 1100 and 1300 RPM
Rated power	370 kW at 1600 RPM

An overview of the steady state engine behavior regarding selected parameters is presented in Figure S7. The calibration of the engine was conducted to maximize the brake efficiency values while considering

the engine-out NO_x emissions targeting current, US10 / Euro VI emissions limits. Accordingly, the peak brake efficiency of the engine is 44 %, which is reached at 1200 RPM and at 200 kW. In this operation range moderate EGR rates are used and the resulting engine-out NO_x emissions are 10 g/kWh.

The appropriate size of the engine was determined by the engine power and torque requirements defined by the USLHC8 drive cycle. Downsizing the engine was considered since engines typically operate more efficiently at high loads. However, downsizing would lead to lower peak power and therefore a larger portion of the engine power demand not being met. Simulations across the USLHC8 were limited to no more than a 1.24 mph average absolute error. The output space of these simulations is depicted in Figure S7. Because 350kW encompasses over 99% of engine power demand with a discrete cutoff, downsizing was not pursued. Hence, the engine max power and torque requirements were determined to be least 350kW and 2000Nm.

A conventional US10 / Euro VI exhaust aftertreatment (EAT) system consists of a diesel oxidation catalyst, a particulate filter, a urea doser, a Selective Catalytic Reduction (SCR) catalyst and an ammonia slip catalyst. An EAT system of this kind has a significant throttling effect downstream the turbine and, thus, increases the pressure level after the turbine – typically leading to a drop in Brake Thermal Efficiency (BTE). Although an EAT system model is not directly included in the diesel Truck Model, its negative effect on BTE is considered in the engine maps (e.g. regarding BTE). Furthermore, using the above mentioned EAT layout ensures compliance with US10/Euro VI emission limits as shown also by the authors in previous works [51, 52, 53].

The engine control unit was implemented to decrease fuel consumption by mediating engine idling and fuel cutting. Fuel cut occurs one second after coasting and fuel resume occurs at 700 RPM. Fuel cut also occurs at 2000 RPM to keep the engine from rotating past its max speed.

Power auxiliaries were modeled to generate a negative torque on the engine and include the A/C, pumps, and fans. The average auxiliary power was defined as 5 kW additional to the USLHC8 power demand. An 18-speed manual transmission based on the Eaton Heavy-Duty Super 18 is used in this study. The gear efficiency was assumed constant across all gears and is 0.97. The clutch's maximum static torque is rated at 3000Nm. The transmission control unit (TCU) was implemented in GT-Suite using the TCU-Manual template and functions to execute the shifting schedule.

As described in section 3.1.6, the average curb weight of long-haul class 8 tractors was defined as 19,500 lb and the average payload for class 8b trucks was defined as 40,600 lb. The parameter aerodynamic drag coefficient was defined as 0.6 [33, 54, 55], and the projected frontal area was defined as 9.2 m^2 [55, 56] for an average long-haul class 8 tractor-trailer. The rolling resistance coefficient was assumed to be independent of the vehicle powertrain and defined as 0.007 in accordance with NAP2020. Similar values are reported by Zhao et al. [44].

3.3.2. Shifting Optimization

Simulations were designed to optimize fuel consumption with performance as a constraint. The goal of the shifting strategy is therefore to operate the engine in its most efficient region. Two approaches were considered in designing the shifting strategy. The first approach was based on constant RPM upshifting and downshifting. Downshifting was explored between 600 and 1000 RPM, while upshifting, ranged from 1600 to 2000 RPM. The second approach considered GTSuite's built-in shift schedule generator, which optimizes shifting by considering acceleration potential and fuel consumption in each gear at various vehicle speeds through static analysis. With a shifting strategy set, the final drive and transmission gear ratios were optimized to further improve fuel consumption. The optimization was performed on the top three gear ratios due to the nature of long-haul driving cruising at high vehicle speeds for the majority of operation. The number of top gear ratios was determined using k means clustering for RPM, velocity, torque, and power over the drive cycle. Using the elbow method, the minimum number of clusters and therefore minimum number of top gears was chosen. A case sweep over the top transmissions and final drive ratios was performed to obtain an output space of fuel consumption. The highest fuel consumption from these results was used to find the initial point for optimization while ensuring a global optimum from the optimizer.

3.3.3. Projected Fuel Consumption

This study considered the powertrains of heavy-duty long-haul trucks in three different scenarios: present, mid term and long term. Future fuel consumption is based on the current simulated value, and increases proportionally to the increase in engine peak efficiency and improved fuel consumption of the waste heat

recovery (WHR) system. The current baseline for comparison of engine peak efficiency is 44% . The mid term peak BTE is assumed to be 55% and is based on the DOE project, SuperTruck II [57]. A BTE of 60% is assumed for the long term and is based on projections set by the Department of Energy as stated in their 21st Century Truck Partnership [58], although efficiencies as high as 66.9% have been modeled in the most ideal scenarios [59].

3.4 Diesel Truck Emission Modeling

This study considered greenhouse gas emissions produced during the fuel production process, well to pump (WTP), and emissions from combusting the fuel as the vehicle operates, pump to wheel (PTW). The entire process consisting of fuel production and vehicle operation is known as well to wheel (WTW), and is a primary output of this study.

The Greenhouse gases, Regulated Emissions, and Energy use in Technologies model (GREET) is the primary tool that was used to calculate WTP emission intensities. GREET allows for the customization of production pathways. Ultra-low sulfur diesel $No.2$, renewable diesel, and biodiesel20 (BD20) were considered in this study. All fuel pathways considered emissions from agricultural impacts, land use change, feedstock and co-product transportation, fuel production, fuel distribution, storage and fuel use. The fuel use (PTW) value for diesel was derived from the EIA carbon dioxide emission coefficient at 10.19 $kgCO_{2eq}/gal$ [60], however, this value was offset by carbon fixation for biofuels during the feedstock growing process. The WTW emissions in gCO_{2eq}/mi were therefore calculated as the sum of WTW and WTP deriving from Equations 1 and 2.

$$WTP = 3.79\frac{ED \times EI}{FE} \tag{1}$$

$$PTW = \frac{EC}{FE} \tag{2}$$

Where ED is energy density in kWh/L, EI is emission intensity calculated by GREET in gCO_{2eq}/kWh, FE is the fuel consumption in mi/gal, and EC is the emission coefficient of diesel fuel in $kgCO_{2eq}/gal$.

3.5 Diesel Truck Total Cost to Society Model

This study used a Total Cost to Society (TCS) analysis to combine operating cost, capital cost and the social cost of GHG emissions into a single metric. A discounted cash flow analysis was conducted using an average discount rate of 7%, based on recommendations by the White House's Office of Management and Budget [61]. Assumptions for each cost consideration vary by year and are included in the present, mid term and long term. More details about the techno-economic estimates are provided in Supplementary Information.

3.5.1. Operating Cost

The operating cost was broken down into labor, maintenance & repair, fuel, permits, licenses and insurance. Table 3 lists the cost data for these parameters based on The American Transportation Research Institute (ATRI) [62]. Detailed equations for total operating cost estimates are given in Supplementary Information. Fuel costs depend on the location and its land price, and transport distances from refinery to retail stations. They have been volatile in past years, impacted by pandemic and civil war. This work uses a pre-pandemic average retail price for diesel fuel for the present-day scenario. In 2019, the average price on highway of the ultra-low sulfur diesel was 3.056 $ USD/gallon [63], which accounted for production, distribution and taxes. Average federal and state taxes (0.56 $ USD/gallon) were removed [64], resulting in a with-out-tax fuel cost of 2.5 $ USD/gallon. For the mid and the long term, the diesel cost was taken from the EIA Annual Energy Outlook projections out to 2050 [65]. The present-day cost of renewable diesel was

Table 3: Operating and capital cost parameters

Item	Values in each scenario			Unit	Reference
	Present	Mid term	Long term		
Aftertreatment cost	5782	7297	9118	USD	[68, 69]
Engine price density	34.62	46.41	51.37	USD/kW	[70]
Fuel tank cost	6.00	6.00	6.00	USD/kg	[28]
Maintenance and repair	0.14	0.14	0.14	USD/mi	[62]
Labor	0.69	0.69	0.69	USD/mi	[62]
Tolls	0.03	0.03	0.03	USD/mi	[62]
Permits and licenses	0.02	0.02	0.02	USD/mi	[62]
Insurance	0.07	0.07	0.07	USD/mi	[62]
WHR system (15 kW)	5900	5900	5900	USD	[71]
18-speed automated manual transmission	10250	10250	10250	USD	[72]
Diesel cost	2.50	2.73	3.13	USD/gal	[63, 65]
Renewable diesel cost	3.14	3.43	3.94	USD/gal	[66]
Biodiesel BD20 cost	2.53	2.77	3.17	USD/gal	[67]

based on the plant gate cost added by the average distribution cost reported by NREL [66]. As for biodiesel $BD20$, the fuel cost was based on the DOE's report on alternative fuel prices published in 2020 [67]. We note the projected prices assume sufficient bio-derived feedstock will be available to meet the demand for the renewable; it is unclear if this would actually be the case in 2050 when several sectors including aviation might be demanding large amounts of bio-derived fuels. Taxes and subsidies were excluded from the total cost to society because taxes and subsidies are internal transfers; therefore, they do not contribute to the TCS.

3.5.2. Capital Cost

The capital cost considers engine, exhaust aftertreatment, transmission, waste heat recovery, fuel tank, and glider manufacturing costs. Special attention was given to powertrain components that were assumed to experience major change as time progresses, such as engine and the exhaust aftertreatment. A manufacturing cost for the engine as a function of engine peak power was derived by Argonne's Energy Systems Division in collaboration with the International Council on Clean Transportation (ICCT) [73]. Cost increases due to efficiency gains were taken into consideration and are shown in Figure S12b. The aftertreatment system cost was based on a manufacturing cost analysis performed by the ICCT [68]. For the present-day scenario, the aftertreatment cost as a function of power is depicted in Figure S12a While future emission regulations are uncertain, this paper assumed that the medium and long term efforts to improve exhaust aftertreatment are primarily to meet Euro VII limits. The estimated incremental cost increase of the aftertreatment system for these scenarios is found in [69]. Particularly for the long term scenario, a two SCR-configuration was assumed for the Euro VII emission control system.

3.5.3. Cost of GHG Emissions

The future damages of CO_2 emissions were translated into economic terms through the Social Cost of Carbon (SCC) metric to account for these externalities. The SCC metric translates the negative climate impacts of a ton of CO_2 emitted into a present monetary value [74]. It has been predominantly used for climate policies and regulations in the US, and to define zero-emissions credits in states such as Illinois and New York [75, 76]. This metric is calculated through integrated models that predict CO_2 emission trajectories over time, and its relationship with economic growth, which refer to climate and socio-economic modules in modular frameworks, respectively. They also determine the climate damages associated to these emissions within the damage module and translate them into present values using rates defined within the discounting module [77]. While the SCC is highly dependent on parameters such as time preference, discount

rates and climate sensitivity, it offers a clarifying baseline to underpin cost-benefit analysis of climate actions. In this work, the SSC estimates from the US Government for the years 2020 through 2050 were used [78]. Therefore, the SCC for a metric ton of CO_2 is 51, 62 and 85 in 2020 dollars for the present, mid and long term using an average discount rate of 3%.

4 Results & Discussion

4.1 Drive Cycle Development

4.1.1. Validation

To validate the degree of representativeness relative to the defined national average driving profile for USLHC8, the Kolmogorov-Smirnov (KS) test was used. Figure 3 displays the KS statistics for the USLHC8 and drive cycles commonly used in the literature. A KS score closer to zero indicates a higher degree of representativeness.

The USLHC8 shows a significantly higher representativeness when compared to all other considered drive cycles in terms of both vehicle speed distribution and road grade distribution. Regarding vehicle speed, USLHC8 showed a lower KS test value than HHDDT, HWFET and NESCCAF by approximately 44%, 12% and 32%, respectively. USLHC8 also shows an approximately 23% lower road grade KS statistic than NESCCAF, the only other drive cycle in consideration that consists of both a vehicle speed and road grade trace.

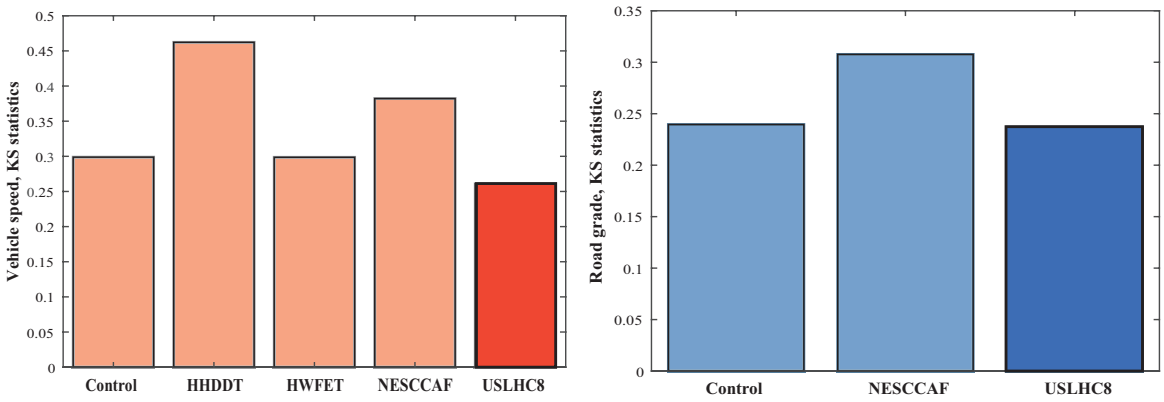

(a) Vehicle speed

(b) Road grade

Figure 3: Two-sample distribution KS statistics of different drive cycles

In addition, the robustness of the generation methodology for USLHC8 was validated. This was done by determining the sensitivity of the KS score to a deviation in the generated drive cycle's error value. The generated Control drive cycle in Figure 3 was selected for its vehicle speed KS score that is very close to the HWFET KS score, which is the second-best after USLHC8. The road grade KS score of Control is about 23 % lower than the NESCCAF KS score. Yet, the Control has an error value which is about 122 % greater than that of the USLHC8. After running the microtrip randomization and evaluation algorithm more than 50 times, the resulting error values only deviated from each other by less than 5%. Therefore, a 122 % increase in the error value is an extremely unlikely result of the algorithm. This demonstrates a very high robustness of the presented methodology in terms of generating drive cycles with a high degree of representativeness relative to the defined national average driving profile. Moreover, the generated degrees of representativeness are consistently higher than those of drive cycles from the literature.

4.1.2. Results

The selected final drive cycle "US Long-Haul Class 8" (USLHC8) is shown in Figure 4, and compared with other drive cycles in Table 4. When considering long-haul driving, USLHC8 has substantial advantages over the other drive cycles in consideration. The USLHC8 covers a total distance of 599.43 miles, has an average vehicle speed of 55.56 mph and a maximum vehicle speed of 70.87 mph, which is the highest vehicle speed of the drive cycles considered. The total driving time at 10 hours and 47 minutes (38840 seconds) is slightly

below the maximum legal driving window of 11 hours. This is crucial to accurately capture prolonged highway driving without too many stops and for powertrain architecture design, because long-haul powertrains must be capable of handling the legal maximum of daily operation. The USLHC8 exhibits a distinguished segment of urban driving at either end. These segments show significantly more acceleration and deceleration as well as lower speed driving. Both urban segments are similar in length at about 2,000 seconds. The urban driving in each segment includes short and interrupted highway sections which model metropolitan traffic and the changing of highways. The remaining long-haul segment in the middle consists of prolonged highway driving which is only interrupted by very few stops. These may represent stops necessary for refueling or the truck operator's personal needs. For the most part, the long-haul segment exhibits steady driving. Two long-haul segments of USLHC8 cover highway speeds at about 55 mph and one segment comprises driving at about 65 mph. The last long-haul segment of USLHC8 also accounts for more transient long-haul driving towards the end of the cycle ranging from about 40 mph to about 70 mph. None of the other drive cycles considered display this inter-metropolitan driving profile representative of long-haul driving in the US. Most USLHC8 road grade values are between -3% and +3%. However, there are also road grade values up to -6% and +6%. Most of these high values are part of the urban segments where extreme grades are more common than on the highway. NESCCAF only demonstrates a synthetic road grade trace limited to 3 %.

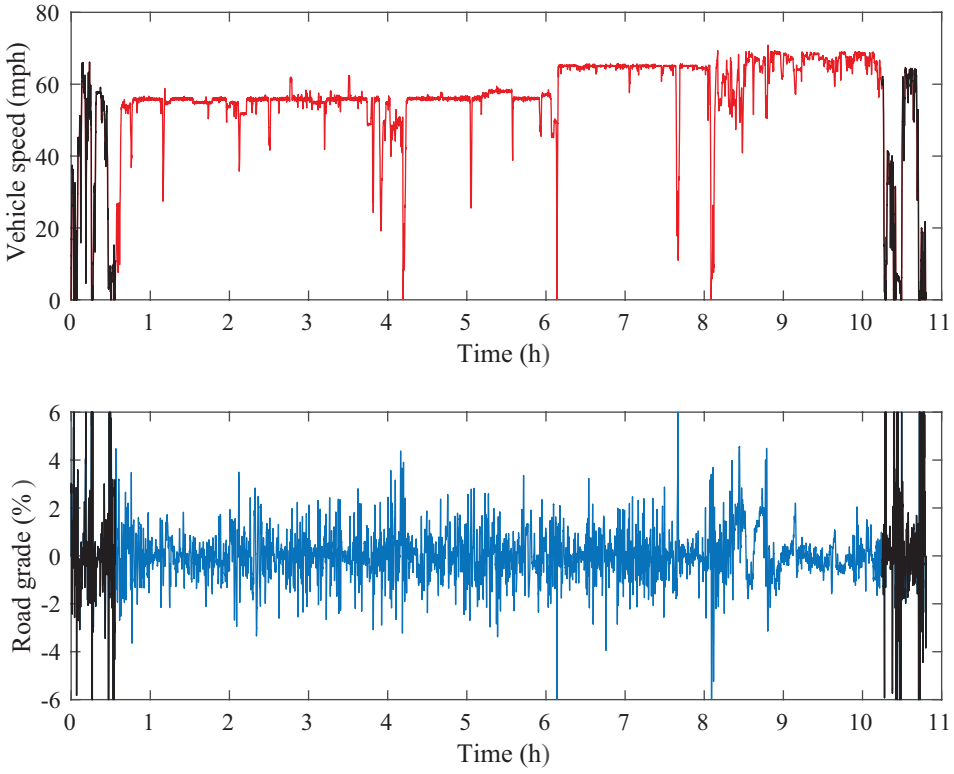

Figure 4: Long-Haul Class 8 Drive Cycle (USLHC8). Urban segments are marked in black

Despite these differences between USLHC8 and drive cycles from the literature, it must also be noted that the overall spread in between the drive cycles is not too large. The USLHC8 vehicle speed KS statistic is about 1.8 standard deviations away from the mean of the literature drive cycle KS statistics. Consequently, it can be concluded that the deviation of USLHC8 from literature drive cycles is within reasonable limits.

In addition to the USLHC8 drive cycle, the drive cycle development methodology itself is discussed in the following. The unique microtrip random generation and evaluation method presented has several distinct advantages over other drive cycle generation methods commonly used in the literature such as k-means microtrip clustering [79] or Markov chains [80, 81]. Most importantly, it allows for the drive cycle to be

Table 4: Properties of USLHC8 and drive cycles commonly used in the literature

Drive cycle	Vehicle speed KS statistic	Road grade KS statistic	Distance (miles)	Time (s)	Average vehicle speed (mph)	Maximum vehicle speed (mph)
HHDDT	0.4622	n.a.	23.07	2084	39.86	59.3
NESCCAF	0.3822	0.3076	72.51	6830	38.22	70.2
HWFET	0.2986	n.a.	10.26	765	48.3	59.9
USLHC8	0.261	0.237	599.43	38840	55.56	70.87

modeled after a specific target vector and not solely to match the average of the base data itself. Also, the microtrip method does not need a validation of driving segments because these consist of measured vehicle speed and road grade traces from actual on-the-road driving. The method also avoids inconsistencies in the generated drive cycles by establishing clear boundary constraints in between concatenated microtrips. Moreover, it allows for a very high variability in generated drive cycles that cannot be achieved using a k-means clustering method. A total number of approximately $1.73*10^{47}$ possible drive cycles significantly increase the likelihood of closely matching the national average driving profile.

4.1.3. Limitations

There are several limitations to the presented work. First and foremost, it must be noted that the presented drive cycle is only intended for modeling and simulation purposes. It is inconveniently long for usage in an experimental setting such as a roller test bench. Another limitation of USLHC8 is the absence of idle time segments, either non-discretionary or discretionary. Non-discretionary idling describes powertrain idling that is not intended by the vehicle operator. Discretionary idling is usually necessary to meet the hotel load energy demand for purposes other than vehicle propulsion. Even though non-discretionary idle time only makes up a negligible part of the energy demand during highway operation [82, 24], it may be significant for determining criteria pollutants and for a more detailed analysis of individual powertrain components. Not accounting for the time the vehicle is stopped in between periods of driving limits the accuracy of powertrain thermal behavior, which may be important for precisely modeling diesel exhaust after-treatment systems, batteries, or fuel cells. A further limitation is that the drive cycle development methodology does not consider vehicle acceleration behavior as an assessment feature and thus USLHC8 might be slightly biased to the ROLR base data. However, no class 8 truck acceleration dataset of sufficient quality could be identified, and the influence of acceleration may be limited during constant speed highway driving. USLHC8 only has a limited amount of prolonged vehicle speed segments above 65 mph, even though the defined national average driving profile incorporates significant driving at vehicle speeds over 70 mph. This is due to limited high vehicle speeds in the ROLR base data and the chosen microtrip method is constrained to the base dataset, since it does not allow for the generation of new synthetic driving segments. Additionally, USLHC8 was chosen from several possible drive cycles generated by the algorithm, which show distinguishable distributions of vehicle speed between individual random sampling. However, they provide relatively close average vehicle speeds and fuel consumption (see SI for details). Despite these limitations, USLHC8 exhibits the highest degree of representativeness to the national average in comparison to all identified drive cycles in the literature.

4.2 Diesel heavy-duty truck model

The engine power distribution of the DICET model over the UCLHC8 drive cycle is shown in Figure 5 and is typically within the range of 70-170 kW. From this power map, the red lines underline the envelope for the majority of potential engine operating points. The optimal fuel economy occurs at 1200 RPM and about 200 kW according to the efficiency map. It is important to clarify that the engine assessed in this work is representative of a typical truck engine on the road today; it does not have the best-in-class fuel

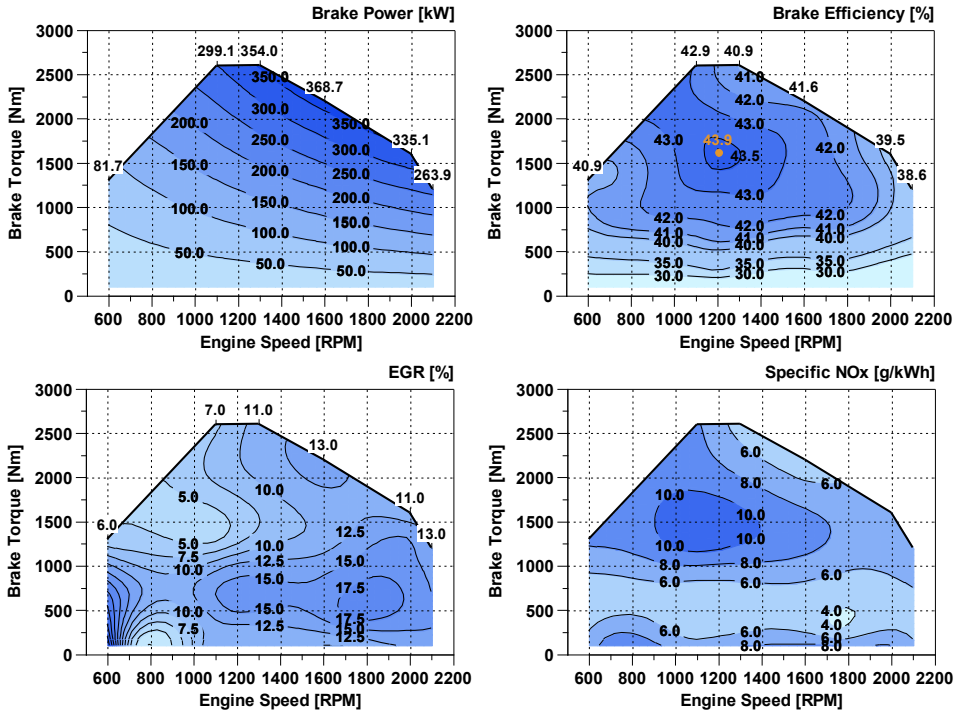

Figure 5: Power and efficiency map of the Diesel engine

consumption efficiency. Several efficiency improvements are achievable with current technology at higher engine cost.

4.2.1. Shifting Optimization

The first optimization approach achieved up to 7.57 mpg by upshifting at 1600 RPM and downshifting at 600 RPM. Figure S8 depicts the fuel consumption ranges at different RPM. The second approach using GT-Suite's optimized shifting algorithm resulted in a fuel consumption of 7.83 mpg. The generated shift schedule is provided in Figure S9. Because the GT-Suite method resulted in lower fuel consumption and satisfied performance constraints, this shifting schedule was used in the final model.

For the case sweep, the top three gears along with the final drive ratio were selected according to the elbow point (see Figure S10). The output space of this optimization is presented as a histogram given in Figure S11. Initial estimates for the optimization of these gears come from the case sweep, where the highest fuel consumption resulted in 7.87 mpg with the gear ratios of 3.1 (final drive), 0.9 (16th gear), 0.86 (17th gear), and 0.75 (18th gear). The optimization was conducted as a minimization of fuel consumption under the constraint of 1.24 mph or smaller mean absolute error relative to the drive cycle vehicle speed trace (equation S2, i.e. we demand that the engine closely meet the power demanded by the drive cycle. The optimization resulted in an optimized fuel consumption value of 7.51 mpg at gear ratios of 3.04 (final drive), 0.82 (16th gear), 0.75 (17th gear), and 0.71 (18th gear) (see Table S5). The operating points with a fuel consumption of 7.10 mpg for the default Eaton-Super18 are shown on the left and operating points with a fuel consumption using the optimized 18 speed transmission are shown on the right in Figure 6.

4.2.2. Modeled Drive Cycle Fuel Consumptions

Table 5 compares the fuel consumption over the DICET model of the USLHC8 and other drive cycles commonly used in the literature.

4.2.3. Sensitivity Analysis

A sensitivity analysis was performed to determine the influence of the input parameters payload, drag coefficient and rolling resistance coefficient on the DICET model fuel consumption. Figure 7 shows the

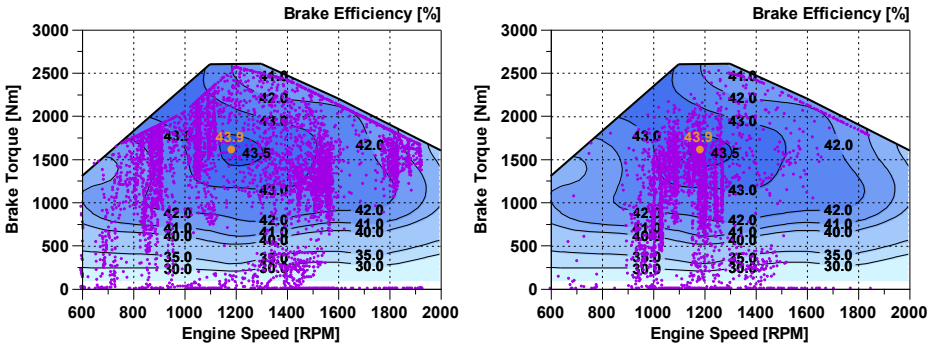

Figure 6: Distribution of operating points for the USLHC8 cycle under two different speed transmission setup: a) default Eaton-Super18 resulting in fuel consumption of 7.10 mpg, and b) optimized gear ratio with fuel consumption of 7.51 mpg

Table 5: Model fuel consumption over literature drive cycles

Drive cycle	Fuel Consumption (in mpg)
USLHC8	7.51
NREL	7.21
HDUDDS	5.70
NESCCAF	7.84
HWFET	7.41

sensitivity relative to the baseline parameters defined in section 3.3.1 and the modeled fuel consumption of 7.51 mpg for the USLHC8 drive cycle. The payload varied from 0 lb, representing an empty truck, to around 60000 lb, representing a fully loaded truck. The upper and lower bounds for the drag coefficient were based on values reported by Sripad et al.[83] for class 8 vehicles. The bounds for frontal area and rolling resistance coefficient were defined according to literature values [32, 83].

Payload had the most significant influence on fuel consumption at 9.95 mpg without load and 6.41 mpg fully loaded. Of course, one does not get paid for running an empty truck. The fuel economy is less sensitive to aerodynamic drag and rolling resistance than it is to payload, but these parameters are still important. Fuel consumption varied from 8.13 mpg to 6.89 mpg when using drag coefficient ranged between 0.5 and 0.7, respectively. The larger this coefficient, the more resistance to motion encountered by the truck and thus more fuel is needed to travel the same mileage. Vehicle frontal area was varied from 8 m^2 to 10 m^2 with resulting fuel consumption of 7.04 mpg and 7.93 mpg, respectively. The coefficient of rolling resistance between 0.006 and 0.008 led to fuel consumption of 7.15 and 7.98 mpg, respectively.

Finally, we considered the effect of including (or not) road grade in the fuel consumption model, since many drive cycles do not take it into account. Road grades impact the power at the wheel required to follow the USLHC8 drive cycle. It influences the total tractive force, primarily the rolling resistance and gravitational components. It was found that the truck travels on average 7.53 miles per gallon of diesel when road grade is excluded from the analysis.

4.2.4. Projected Fuel Efficiency of Trucks in the Future

The calculated fuel consumption for the present-day DICET model running on the USLHC8 drive cycle is 7.51 mpg. Future fuel consumption is projected to be 9.59 mpg for the mid term and 10.46 mpg for the long term. These increases are mainly due to engine improvements, and to the addition of a waste heat recovery unit, as other powertrain components such at the transmission already operate at close to ideal efficiencies. The waste heat recovery system added in the mid and long term scenario improves fuel consumption by powering the auxiliary load using waste heat generated by the engine. Similar improvements in the fuel consumption of diesel long-haul trucks have already been demonstrated in the context of DOE's SuperTruck projects. For example, the Cummins-Peterbilt team reported fuel consumption ranging between 9.2 and

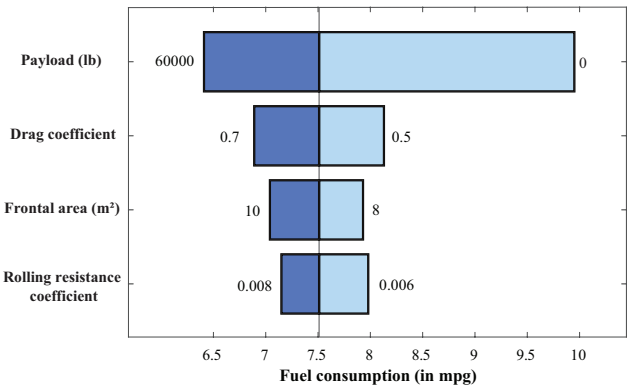

Figure 7: Effect of design parameters on fuel consumption

10.7 mpg in real driving conditions, while the Daimler team achieved a peak fuel consumption of 12.2 mpg [84]. Recent publications have also projected advances in present-day technologies that lead to higher freight efficiencies and better diesel engine performance. For instance, Tong et al.[85] estimated advances in fuel consumption of 20 % to 41 % for different designs of long-haul diesel trucks with modifications in empty vehicle weight, rolling resistance and frontal area.

4.3 Well to Wheel Emissions

Figure 8 shows the computed greenhouse gas emissions associated with fuel production (WTP) and fuel combustion during use (PTW) for the diesel long-haul truck. Using conventional diesel led to WTW emissions of 1507, 1180 and 1081 gCO_2/mi for the present, mid and long term, respectively. Since WTW emissions are highly dependent on vehicle models, design attributes, assumed payload, and drive cycles, a wide range of values is found in the literature for diesel powertrains. Several other authors have recently estimated GHG emissions from trucking, reporting slightly higher values, e.g. in 2021 Liu et al.[86] obtained a value of 1846 gCO_2/mi, and in 2015 Camuzeaux et al. [87] computed a value close to 2000 gCO_2/mi.

Renewable diesel has the lowest emissions followed by biodiesel BD20; because all the carbon in renewable diesel is non-fossil in origin, absorbed from the atmosphere by growing plants, it is not counted as a GHG emission. However, it is not zero-emission, since significant greenhouse gases are emitted to grow and harvest the plants, to convert them into fuel, and in transporting both the biomass and the finished fuel.

4.4 Total Cost to Society

The capital cost for the present, mid term, and long term slightly increase over time and are roughly 125,400, 137,000, and 140,500 USD (see Figure 9). The glider makes up the majority of the capital cost at 95,000 USD and was included to account for the total capital cost. However, the analysis focused on powertrain components and their cost variation over time. The largest powertrain cost is attributed to the engine.

The engine cost is 12,000 USD in 2020 and increases to nearly 18,000 USD in the mid term projection. This increase is due to technology improvements to meet emission requirements and increase fuel consumption [88]. In particular, the waste heat recovery system increases the capital cost by 6,000 USD [71], however, this value would be lower in mass production. Also included in the capital cost are the fuel tank, transmission, exhaust aftertreatment system, and battery.

Figure 10 shows the operating cost for each diesel fuel type and time scenarios. For trucking operations in the USA, labor is the largest operating cost component followed by fuel, maintenance and repair, insurance,

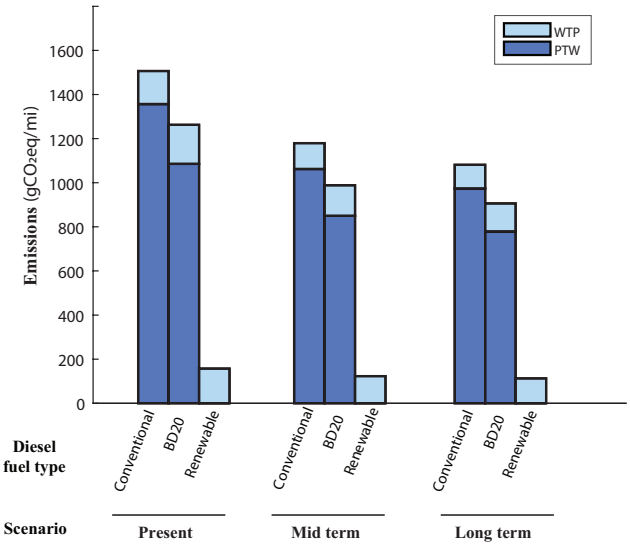

Figure 8: Total Well to Wheel emissions

and fees. Labor costs are assumed to be constant in these calculations, but this is quite uncertain. Salaries may increase faster than inflation, causing real labor costs to rise, or labor costs might drastically decrease in the long term if autonomous driving is widely deployed. The scope of this study is limited to variations in powertrain and fuel cost.

The price of all fuels is expected to increase over time per the EIA's projections (though this is quite uncertain, e.g. subject to future decisions by OPEC and by the USA government). The fuel efficiency increase from engine improvements is expected to partially offset the increase in fuel price. Renewable diesel is associated with the largest operating cost in all scenarios, followed by conventional diesel, and BD20. While renewable diesel as a drop-in fuel drastically cuts emissions, it is more expensive than BD20 or conventional diesel. These price differences among diesel fuel types come from both production and supply factors. The production of renewable diesel is currently lower than biodiesel in the USA, and the majority of its capacity is located on the West Coast; supplying this fuel to other farther regions adds more distribution costs. There is also a finite supply of the vegetable oils from which these biofuels are made; that limit is likely to become important in the long term.

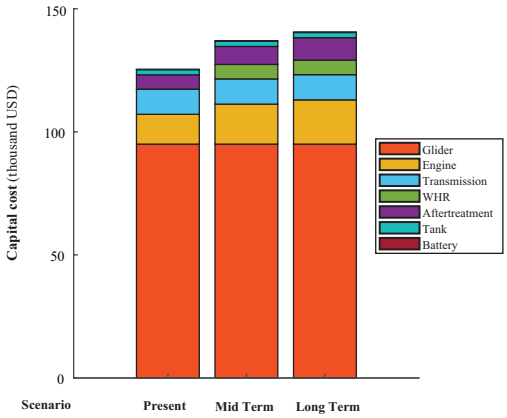

Figure 9: Capital costs per truck

A recent comprehensive total cost of ownership analysis was performed by Argonne National Laboratory (ANL) [88]. The results of this study are compared to the ANL results in Figure 11. The ANL model considers additional costs relative to the DICET model including taxes and financing over time. Taxes are not included within the DICET model because the model will serve as a comparison baseline to alternative powertrains, where the extent and methodology of future taxation are largely uncertain. When equipping the DICET model with ANL parameters, results are within 5% of each other. The DICET model with our parameters differs from the ANL model with ANL parameters by roughly 30%. Major differences in input parameters include the discount factor, fuel consumption, and diesel price. The ANL model used a discount factor of 3%, whereas the DICET model uses 7%. The fuel consumption per mile used within the ANL model is nearly 15% different than the value computed here using the DICET model. This difference is attributed to different driving patterns. The ANL model considered all class 8 trucks, while the DICET model focused strictly on long-haul operation. We noted in section 3.5.1 that fuel prices depend on location and have been volatile in past years. The diesel costs in the ANL model were 3.08 and 3.37$ USD/gallon, with fuel taxes

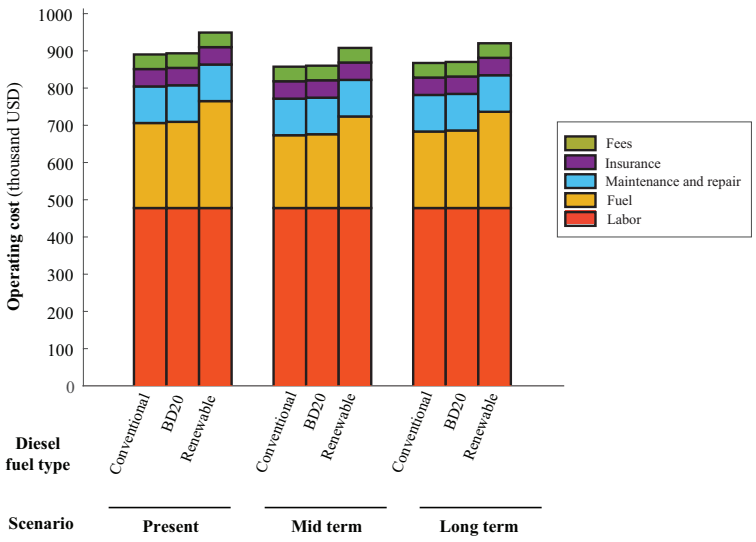

Figure 10: Operating costs per truck, lifetime

included, which constitutes 22% of the final diesel cost. As stated, the DICET model removes the diesel tax to facilitate comparison to alternative powertrain and fuel combinations on a "total cost to society" basis.

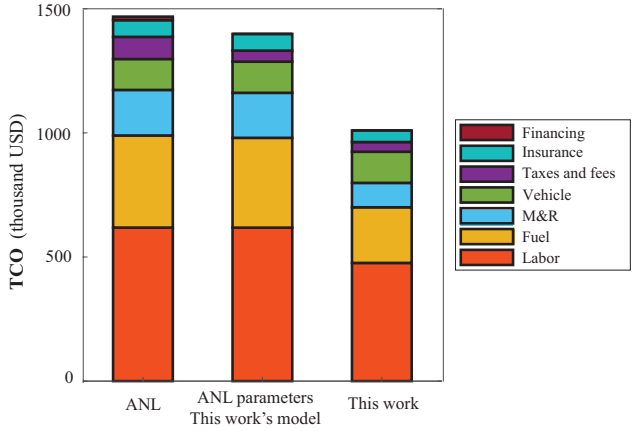

Figure 11: Comparison of total cost of ownership results with other works

Figure 12 shows the total cost to society of the diesel powertrain for each diesel fuel type. The social cost of carbon penalizes emissions more severely in the later years. The social cost of carbon values used here are insufficient to offset the significantly higher operating (fuel) cost when renewable diesel is used instead of conventional (fossil) diesel fuel.

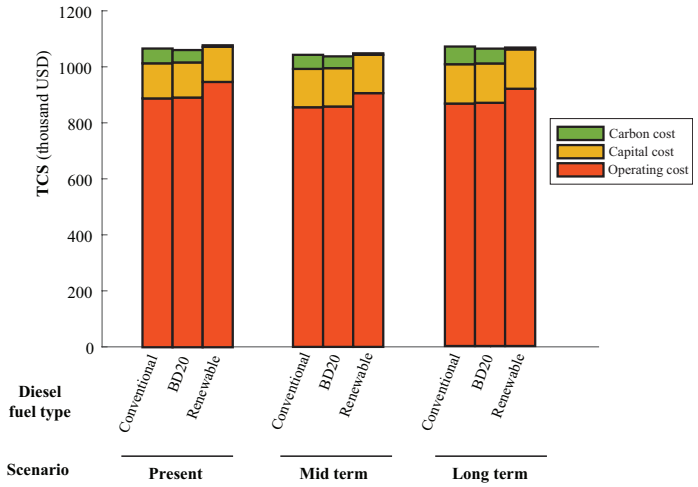

Figure 12: Total Cost to Society per truck, lifetime

5 Conclusion

Long-haul heavy-duty trucks constitute the backbone of growing US freight transport but are also responsible for a large fraction of transport-related greenhouse gas emissions.

Various alternative truck powertrains have been assessed to reduce these freight transport emissions. In the reviewed literature, consensus on the best powertrain solution has not yet been found. This is likely due to widely varying assumptions, including the use of drive cycles with significant shortcomings in terms of representing actual long-haul operations in the US. The main shortcomings are a lack of appropriate vehicle speed transients, realistic road grades, and maximum vehicle speeds.

To allow for an accurate comparison of alternative powertrains on a consistent basis, this paper defines a drive cycle that represents how long-haul trucks are actually driven in the USA. The USLHC8 drive cycle was developed using a unique microtrip random selection algorithm, and many hours of real-world driving data covering 58,000 miles. The drive cycle was sampled from many possible drive cycles generated with the algorithm, featuring a high degree of representativeness. It consists of a vehicle speed and road grade trace and covers a total distance of 599.43 miles with an average vehicle speed of 55.56 mph. Compared to drive cycles in the reviewed literature, it has a higher degree of representativeness to the national average driving profile. USLHC8 was successfully validated using Kolmogorov-Smirnov statistics.

USLHC8 and a simulation of a modern diesel engine served as the main inputs for a system-level simulation of the diesel powertrain. The simulation includes power auxiliaries, an exhaust aftertreatment system, as well as an optimized transmission and shifting strategy. Based on the simulation and USLHC8, well-to-wheel emissions were calculated to be 1507 gCO_2 per mile for conventional diesel. The majority of these emissions were pump-to-wheel emissions, which were zero for renewable diesel. Emissions and fuel consumption were projected to steadily decrease over time as truck technology improves. Using the social cost of carbon, CO_2 emissions and total cost of ownership were combined into a single metric, the Total Cost to Society (TCS). The TCS of purchasing and operating a truck over its lifetime was calculated for conventional diesel, renewable diesel, and biodiesel BD20 while projected under current, mid, and long-term scenarios. Renewable diesel had the highest TCS, followed by BD20 and conventional diesel. The TCS was projected to steadily increase over time for all diesel fuel types despite projected improvements in efficiency, due to rising fuel prices. Finally, the results of the TCS were successfully validated against the literature.

Nevertheless, several limitations to the presented research have to be taken into account. First, the drive cycle USLHC8 is only intended for modeling and simulation purposes and is not designed to be convenient for practical engine testing. USLHC8 also does not consider idle time segments, which limits the modeling

accuracy of powertrain thermal behavior and hotel load power demand. Concerning the diesel powertrain simulation, the transmission design and gear-shift optimization were specific to USLHC8. Therefore, optimal performance would be different in simulations with other cycles. Lastly, both labor and fuel costs in the TCS analysis are highly uncertain in future scenarios and can be greatly affected by political and economic instability and future regulations; all of these are factors outside the scope of this paper.

The supplementary parameter definition and drive cycle development presented in this paper complement the literature with the first publicly available comprehensive characterization of the US long-haul class 8 truck driving profile. Furthermore, the results of the diesel model and total cost to society analysis provide a consistent benchmark for future research to compare alternative powertrain solutions in the present, mid term, and long term. Taken together, this paper enables a substantially more accurate comparison of long-haul powertrains in terms of their cost and greenhouse gas emissions. Based thereon, stakeholders like manufacturers, investors, and policymakers, may be presented with less uncertainty about the optimal powertrain solution for the long-haul sector, allowing for better decisions.

Since long-haul truck deliveries make up over 70 % of the continuously growing US freight sector, the presented research has the potential to make a significant contribution to improving the US economy and accelerating national decarbonization.

6 Acknowledgement

The authors thank Marian Mennig for helpful discussions with regard to engine modeling. We would also like to acknowledge MathWorks for Kariana Moreno's engineering fellowship. This work was financially supported by the MIT Mobility Systems Center consortium, an MIT Energy Initiative Low-Carbon Energy Center.

7 Author Contribution Statement

The authors confirm contribution to the paper as follows: study conception and design: R. Jones, M. Köllner, and W.H. Green; data collection: R. Jones, M. Köllner, D. Kovács, T. Delebinski, and R. Rezaei; analysis and interpretation of results: R. Jones, M. Köllner, K. Moreno-Sader, D. Kovács and W.H. Green; draft manuscript preparation: R. Jones, M. Köllner, K. Moreno-Sader, and W.H. Green. All authors reviewed the results and approved the final version of the manuscript.

References

[1] U.S. Environmental Protection Agency. Sources of greenhouse gas emissions, 2018. URL https://www.epa.gov/ghgemissions/sources-greenhouse-gas-emissions.

[2] Stacy C Davis and Robert G Boundy. Transportation energy data book: Edition 37.2, 2019. ISSN 10563466.

[3] U.S. Department of Transportation. Bureau of Transportation Statistics. 2017 cfs preliminary data. u.s. department of transportation, 2018. URL https://www.bts.gov/surveys/commodity-flow-survey/2017-cfs-preliminary-data.

[4] Freight Analysis Framework. Faf trend - over time (1997 - 2045), 2012. URL https://explore.dot.gov/views/FAF_Dashboard_451/.

[5] Bureau of Transportation Statistics. National transportation statistics 9/4/19 update, shares of u.s. energy consumption and other categories, 2019. URL https://www.bts.gov/newsroom/national-transportation-statistics-9419-update-shares-us-energy-consumption-and-other.

[6] EPA. Regulations for greenhouse gas emissions from commercial, 2022. URL https://www.epa.gov/regulations-emissions-vehicles-and-engines/regulations-greenhouse-gas-emissions-commercial-trucks.

[7] Philip Leistner, Aleksandar Lozanovski, Oliver Dingel, and Matthias Erath. Environmental impact of various "co2 neutral" long-haul heavy- duty powertrains, 2020.

[8] Ana Guerrero de la Peña, Navindran Davendralingam, Ali K. Raz, Daniel DeLaurentis, Gregory Shaver, Vivek Sujan, and Neera Jain. Projecting adoption of truck powertrain technologies and co2 emissions in line-haul networks. *Transportation Research Part D: Transport and Environment*, 84, 7 2020. ISSN 13619209. doi: 10.1016/j.trd.2020.102354.

[9] S. Mojtaba Lajevardi, Jonn Axsen, and Curran Crawford. Simulating competition among heavy-duty zero-emissions vehicles under different infrastructure conditions. *Transportation Research Part D: Transport and Environment*, 106: 103254, 5 2022. ISSN 13619209. doi: 10.1016/j.trd.2022.103254. URL https://linkinghub.elsevier.com/retrieve/pii/S1361920922000840.

[10] S. Mojtaba Lajevardi, Jonn Axsen, and Curran Crawford. Examining the role of natural gas and advanced vehicle technologies in mitigating co2 emissions of heavy-duty trucks: Modeling prototypical british columbia routes with road grades. *Transportation Research Part D: Transport and Environment*, 62:186–211, 7 2018. ISSN 13619209. doi: 10.1016/j.trd.2018.02.011.

[11] U.S. Environmental Protection Agency. Vehicle and fuel emissions testing: Dynamometer drive schedules, 2021. URL https://www.epa.gov/vehicle-and-fuel-emissions-testing/dynamometer-drive-schedules.

[12] Dieselnet. Heavy heavy-duty diesel truck (hhddt) schedule, 2007. URL https://dieselnet.com/standards/cycles/hhddt.php.

[13] NESCCAF Northeast States Center for a Clean Air Future; ICCT International Council on Clean. Heavy-duty long haul combination truck fuel consumption and co 2 emissions, 2009.

[14] Chen Zhang, Andrew Kotz, Kenneth Kelly, and Luke Rippelmeyer. Development of heavy-duty vehicle representative driving cycles via decision tree regression. *Transportation Research Part D: Transport and Environment*, 95:102843, 2021. ISSN 1361-9209. doi: https://doi.org/10.1016/j.trd.2021.102843. URL https://www.sciencedirect.com/science/article/pii/S1361920921001462.

[15] American Trucking Association. Truck driver shortage analysis 2019. *American trucking association*, 2019. ISSN 1098-6596.

[16] Stephen V Burks and Kristen Monaco. Is the u.s. labor market for truck drivers broken? *Monthly Labor Review*, 2019: 1–21, 2019. ISSN 19374658. doi: 10.21916/mlr.2019.5.

[17] Eric Wood, Adam Duran, and Kenneth Kelly. Epa ghg certification of medium- and heavy-duty vehicles: Development of road grade profiles representative of us controlled access highways. *SAE International Journal of Fuels and Lubricants*, 9, 2016. ISSN 19463960. doi: 10.4271/2016-01-8017.

[18] Dong Yeon Lee, Amgad Elgowainy, Andrew Kotz, Ram Vijayagopal, and Jason Marcinkoski. Life-cycle implications of hydrogen fuel cell electric vehicle technology for medium- and heavy-duty trucks. *Journal of Power Sources*, 393:217–229, 2018. ISSN 03787753. doi: 10.1016/j.jpowsour.2018.05.012. URL https://doi.org/10.1016/j.jpowsour.2018.05.012.

[19] Liam Langshaw, Daniel Ainalis, Salvador Acha, Nilay Shah, and Marc E.J. Stettler. Environmental and economic analysis of liquefied natural gas (lng) for heavy goods vehicles in the uk: A well-to-wheel and total cost of ownership evaluation. *Energy Policy*, 137, 2 2020. ISSN 03014215. doi: 10.1016/j.enpol.2019.111161.

[20] U.S. DOE. Compressed natural gas fueling stations, 2021. URL https://afdc.energy.gov/fuels/natural_gas_cng_stations.html.

[21] Freightliner. Freightliner ecascadia: Specs & resources, 2021. URL https://freightliner.com/trucks/ecascadia/.

[22] U.S. DOE. Most common maximum speed limit for trucks in 2017 was 70 miles per hour, 2019. URL https://www.energy.gov/eere/vehicles/articles/fotw-1075-april-1-2019-most-common-maximum-speed-limit-trucks-2017-was-70.

[23] Kanok Boriboonsomsin, Kent Johnson, George Scora, Daniel Sandez, Alexander Vu, Tom Durbin, and Yu Jiang. Collection of activity data from on-road heavy-duty diesel vehicles collection of activity data from on-road heavy-duty diesel vehicles final report, 2017.

[24] Rick Mihelic, David Schaller, Yunsu Park, Kevin Otto, Mike Roeth, and Denise Rondini. Run on less regional report, 2020.

[25] J Damasky. Antriebe der zukunft für pkw und nfz aus vda sicht, 2019.

[26] Global Green Freight. Long-haul, 2021. URL http://www.globalgreenfreight.org/transport-modes/land/road/long-haul.

[27] Andrew Burnham, David Gohlke, Luke Rush, Thomas Stephens, Yan Zhou, Mark A Delucchi, Alicia Birky, Chad Hunter, Zhenhong Lin, Shiqi Ou, Fei Xie, Camron Proctor, Steven Wiryadinata, Nawei Liu, and Madhur Boloor. Comprehensive total cost of ownership quantification for vehicles with different size classes and powertrains. *U.S. Department of Energy,*

Argonne National Laboratory, 2021. URL https://publications.anl.gov/anlpubs/2021/05/167399.pdf.
[28] Marissa Moultak, Nic Lutsey, and Dale Hall. Transitioning to zero-emission heavy-duty freight vehicles, 9 2017. URL https://theicct.org/sites/default/files/publications/Zero-emission-freight-trucks_ICCT-white-paper_26092017_vF.pdf.
[29] California Air Resource Board. Heavy-duty omnibus regulation, 2021. URL https://ww2.arb.ca.gov/rulemaking/2020/hdomnibuslownox.
[30] Ram Vijayagopal, D Nieto Prada, A Rousseau, and Luz Yolanda Toro Suarez. Fuel economy and cost estimates for medium- and heavy-duty trucks. *U.S. Department of Energy, Argonne National Laboratory*, 2019.
[31] Mark Kuhn. Valuation of fuel economy of medium duty/heavy duty vehicles, 2017. URL https://cdn.ricardo.com/rsc/media/assets/ricardo-md_hd-technology-valuation-study-white-paper-20170613.pdf.
[32] Lukas Mauler, Laureen Dahrendorf, Fabian Duffner, Martin Winter, and Jens Leker. Cost-effective technology choice in a decarbonized and diversified long-haul truck transportation sector: A u.s. case study. *Journal of Energy Storage*, 46, 2 2022. ISSN 2352152X. doi: 10.1016/j.est.2021.103891.
[33] Hengbing Zhao, Qian Wang, Lewis Fulton, Miguel Jaller, and Andrew Burke. A comparison of zero-emission highway trucking technologies, 10 2018. URL https://orcid.org/0000-0002-4245-0056.
[34] Dan Murray and Seth Glidewell. An analysis of the operational costs of trucking: 2019 update, 11 2019. URL https://truckingresearch.org/wp-content/uploads/2019/11/ATRI-Operational-Costs-of-Trucking-2019-1.pdf.
[35] Thomas Zabelsky, John Miller, Ruth Detlefsen, Bernard Fitzpatrick, Dennis Stoudt, Barry Sessamen, and Robert Brown. 2002 economic census: Vehicle inventory and use survey, 12 2004. URL https://www2.census.gov/library/publications/economic-census/2002/vehicle-inventory-and-use-survey/ec02tv-us.pdf.
[36] Federal Motor Carrier Safety Administration. Summary of hours of service regulations, 3 2022. URL https://www.fmcsa.dot.gov/regulations/hours-service/summary-hours-service-regulations.
[37] Frank Pietras, Matthias Ermer, Matthieu Simon, and Benny Guttmann. Trends in the truck & trailer market. *Roland Berger*, 2018. URL https://www.rolandberger.com/publications/publication_pdf/roland_berger_trends_trucks_trailer.pdf.
[38] Jason Marcinkoski, Ram Vijayagopal, Jesse Adams, Brian James, John Kopasz, and Rajesh Ahluwalia. Doe advanced truck technologies: Technical targets for hydrogen-fueled long-haul tractor-trailer trucks. *Electrified Powertrain Roadmap*, 2019.
[39] National Research Council of the National Academies. Technologies and approaches to reducing the fuel consumption of medium- and heavy-duty vehicles, 2010.
[40] Eran Sher. *Handbook of air pollution from internal combustion engines. Pollutant formation and control*. Academic Press, 1st edition edition, 3 1998. ISBN 9788578110796.
[41] Penske ExpressLease. 2011 freightliner cascadia 113, 2021. URL https://www.pensketruckleasing.com/pdfs/Freightliner_Cascadia-113.pdf.
[42] M Smith and C Eberle. Heavy vehicle mass reduction goals and manufacturing challenges. presentation at the u.s. department of energy workshop on tooling technology for low volume vehicle production, 2003.
[43] U.S. Environmental Protection Agency. Smartway program, 2021. URL https://www.epa.gov/smartway.
[44] Hengbing Zhao, Andrew Burke, and Marshall Miller. Analysis of class 8 truck technologies for their fuel savings and economics. *Transportation Research Part D: Transport and Environment*, 2013. ISSN 13619209. doi: 10.1016/j.trd.2013.04.004.
[45] Tim LaClair. Application of a tractive energy analysis to quantify the benefits of advanced efficiency technologies for medium- and heavy-duty trucks using characteristic drive cycle data. *SAE Technical Papers*, 5, 2012. ISSN 26883627. doi: 10.4271/2012-01-0361.
[46] Yunsu Park, Mike Roeth, Denise Rondini, David Schaller, and Bianca Wachtel. Run on less report, 2018.
[47] Gary Capps, Oscar Franzese, Bill Knee, Mary Beth Lascurain, and Pedro Otaduy. Class-8 heavy truck duty cycle project final report no. ornl/tm-2008/122, 12 2008. URL http://www.osti.gov/bridge.
[48] K Walkowicz, K Kelly, A Duran, and E Burton. Fleet dna project data, 2019.
[49] TomTom N.V. Tomtom adas map, 2021. URL https://www.tomtom.com/products/adas-map/.
[50] Oscar Delgado, Felipe Rodriguez, and Rachel Muncrief. Fuel efficiency technology in european heavy-duty vehicles: Baseline and potential for the 2020-2030 timeframe, 2017. URL www.theicct.org.
[51] H. Rauch, D. Kovács, R. Rezaei, V. Strots, S. Kah, and A. Wille. Two-stage scr system for commercial vehicle applications, 2018.
[52] David Kovacs, Marian Mennig, Reza Rezaei, and Christoph Bertram. Holistic engine and eat development of low nox and co2 concepts for hd diesel engine applications. *SAE International Journal of Advances and Current Practices in Mobility*, 3:320–336, 9 2020. ISSN 2641-9637. doi: https://doi.org/10.4271/2020-01-2092. URL https://doi.org/10.4271/2020-01-2092.
[53] Hendrik Rauch, Reza Rezaei, Martin Weber, David Kovacs, Vadim Strots, and Christoph Bertram. Holistic development of future low nox emission concepts for heavy-duty applications, 2018. ISSN 01487191.
[54] Randall Guensler, Seungju Yoon, Chunxia Feng, Hainan Li, and Jungwook Jun. Heavy-duty diesel vehicle modal emission model (hddv-mem) volume i: Modal emission modeling framework, 8 2005. URL https://cfpub.epa.gov/si/si_public_record_Report.cfm?Lab=NRMRL&dirEntryId=137904.
[55] The National Academies of Science Engineering and Medicine. Reducing fuel consumption and greenhouse gas emissions of medium- and heavy-duty vehicles, phase two, 2019.
[56] 21st Century Truck Partnership. Roadmap and technical white papers, 2 2013. URL https://www1.eere.energy.gov/vehiclesandfuels/pdfs/program/21ctp_roadmap_white_papers_2013.pdf.
[57] U.S. Department of Energy. Super truck 2, 6 2021. URL https://www.energy.gov/eere/vehicles/articles/supertruck-2-paccar.
[58] 21st Century Truck Partnership. Research blueprint, 2 2019.

[59] Jerald A Caton. Maximum efficiencies for internal combustion engines: Thermodynamic limitations. *International Journal of Engine Research*, 19:1005–1023, 2018. doi: 10.1177/1468087417737700. URL https://doi.org/10.1177/1468087417737700.

[60] U.S. Energy Information Administration. Carbon dioxide emissions coefficients, 2022. URL https://www.eia.gov/environment/emissions/co2_vol_mass.php.

[61] Office of Management and Budget. Discount rates for cost-effectiveness analysis of federal programs, 12 2020. URL https://www.federalregister.gov/documents/2020/12/29/2020-28650/discount-rates-for-cost-effectiveness-analysis-of-federal-programs.

[62] Nathan Williams and Dan Murray. An analysis of the operational costs of trucking: 2020 update, 11 2020. URL https://truckingresearch.org/wp-content/uploads/2020/11/ATRI-Operational-Costs-of-Trucking-2020.pdf.

[63] U.S. Energy Information Administration. Weekly retail gasoline and diesel prices, 2020. URL https://www.eia.gov/dnav/pet/PET_PRI_GND_DCUS_NUS_A.htm.

[64] U.S. Energy Information Administration. Federal and state motor fuel taxes, 2020. URL https://www.eia.gov/petroleum/marketing/monthly/.

[65] U.S. Energy Information Administration. Annual energy outlook 2021 with projections to 2050, 2021. ISSN 1387-1811. URL https://www.eia.gov/outlooks/aeo/data/browser/#/?id=12-AEO2021&region=0-0&cases=ref2021&start=2019&end=2050&f=A&linechart=~ref2021-d113020a.32-12-AEO2021&map=&ctype=linechart&sourcekey=0.

[66] National Renewable Energy Laboratory. Diesel fuel, 2020. URL https://atb.nrel.gov/transportation/2020/diesel_fuel.

[67] U.S. Department of Energy. Clean cities alternative fuel price report, january 2020, 2020. URL https://afdc.energy.gov/files/u/publication/alternative_fuel_price_report_jan_2020.pdf.

[68] Francisco Posada, Sarah Chambliss, and Kate Blumberg. Costs of emissions reduction technologies for heavy-duty diesel vehicles, 2 2016. URL https://theicct.org/sites/default/files/publications/ICCT_costs-emission-reduction-tech-HDV_20160229.pdf.

[69] Pierre-Louis Ragon and Felipe Rodríguez. Estimated cost of diesel emissions control technology to meet future euro vii standards, 2021. URL www.theicct.org.

[70] Argonne National Laboratory. Anl-mdhd vehicle simulation, 2022. URL https://www.autonomie.net/pdfs/ANL-MDHDVehicleSimulationReport.pdf.

[71] John Norris and Giulia Escher. Heavy duty vehicles technology potential and cost study, 4 2017. URL https://theicct.org/sites/default/files/publications/HDV-Technology-Potential-and-Cost-Study_Ricardo_Consultant-Report_26052017_vF.pdf.

[72] S Mojtaba Lajevardi, Jonn Axsen, Curran Crawford, S Mojtaba Lajevardi, Jonn Axsen, Curran Crawford, S Mojtaba Lajevardi, Jonn Axsen, Curran Crawford, S Mojtaba Lajevardi, Jonn Axsen, Curran Crawford, S Mojtaba Lajevardi, Jonn Axsen, and Curran Crawford. Comparing alternative heavy-duty drivetrains based on ghg emissions, ownership and abatement costs: Simulations of freight routes in british columbia. *Transportation Research Part D: Transport and Environment*, 76, 2019. ISSN 13619209. doi: 10.1016/j.trd.2019.08.031. URL https://doi.org/10.1016/j.trd.2019.08.031.

[73] T Stephens, R Vijayagopal, M Dwyer, A Birky, and A Rousseau. Vehicle technologies and fuel cell technologies office research and development programs: Prospective benefits assessment for medium-and heavy-duty vehicles, 11 2019.

[74] Gernot Wagner, David Anthoff, Maureen Cropper, Simon Dietz, Kenneth T Gillingham, Ben Groom, J Paul Kelleher, Frances C Moore, and James H Stock. Eight priorities for calculating the social cost of carbon, 2021.

[75] Tamma Carleton and Michael Greenstone. Updating the united states government's social cost of carbon, 11 2021.

[76] Peter Fairley. States are using social cost of carbon in energy decisions, despite trump's opposition, 8 2017. URL https://insideclimatenews.org/news/14082017/states-climate-change-policy-calculate-social-cost-carbon/.

[77] Katharine Ricke, Laurent Drouet, Ken Caldeira, and Massimo Tavoni. Country-level social cost of carbon. *Nature Climate Change*, 8:895–900, 10 2018. ISSN 17586798. doi: 10.1038/s41558-018-0282-y.

[78] Interagency Working Group on Social Cost of Greenhouse Gases. Technical support document: Social cost of carbon, methane, and nitrous oxide interim estimates under executive order 13990, 2021. URL https://www.whitehouse.gov/wp-content/uploads/2021/02/TechnicalSupportDocument_SocialCostofCarbonMethaneNitrousOxide.pdf.

[79] A. Fotouhi and M. Montazeri-Gh. Tehran driving cycle development using the k-means clustering method. *Scientia Iranica*, 20:286–293, 2013. ISSN 10263098. doi: 10.1016/j.scient.2013.04.001.

[80] Levente Czégé, Attila Vámosi, and Imre Kocsis. Review on Construction Procedures of Driving Cycles. *International Journal of Engineering and Management Sciences*, 5(2), 2020. doi: 10.21791/ijems.2020.2.31.

[81] H. Y. Tong and W. T. Hung. A framework for developing driving cycles with on-road driving data. *Transport Reviews*, 30:589–615, 2010. ISSN 14645327. doi: 10.1080/01441640903286134.

[82] Tim Laclair, Zhiming Gao, Adam Siekmann, Joshua Fu, Jimmy Calcagno, and Jeongran Yun. Truck technology efficiency assessment (ttea) project final report, 10 2012. URL http://info.ornl.gov/sites/publications/files/Pub40546.pdf.

[83] Shashank Sripad and Venkatasubramanian Viswanathan. Performance metrics required of next-generation batteries to make a practical electric semi truck. *ACS Energy Letters*, 2(7):1669–1673, 2017. doi: 10.1021/acsenergylett.7b00432. URL https://doi.org/10.1021/acsenergylett.7b00432.

[84] Zhiming Gao, David E. Smith, C. Stuart Daw, K. Dean Edwards, Brian C. Kaul, Norberto Domingo, James E. Parks, and Perry T. Jones. The evaluation of developing vehicle technologies on the fuel economy of long-haul trucks. *Energy Conversion and Management*, 106:766–781, 12 2015. ISSN 01968904. doi: 10.1016/j.enconman.2015.10.006.

[85] Fan Tong, Alan Jenn, Derek Wolfson, Corinne D. Scown, and Maximilian Auffhammer. Health and climate impacts from long-haul truck electrification. *Environmental Science and Technology*, 55:8514–8523, 7 2021. ISSN 15205851. doi: 10.1021/acs.est.1c01273.

[86] Xinyu Liu, Amgad Elgowainy, Ram Vijayagopal, and Michael Wang. Well-to-wheels analysis of zero-emission plug-in battery electric vehicle technology for medium- and heavy-duty trucks. *Environmental Science and Technology*, 55:538–

546, 1 2021. ISSN 15205851. doi: 10.1021/acs.est.0c02931.

[87] Jonathan R. Camuzeaux, Ramón A. Alvarez, Susanne A. Brooks, Joshua B. Browne, and Thomas Sterner. Influence of methane emissions and vehicle efficiency on the climate implications of heavy-duty natural gas trucks. *Environmental Science and Technology*, 49:6402–6410, 6 2015. ISSN 15205851. doi: 10.1021/acs.est.5b00412.

[88] Andrew Burnham, David Gohlke, Luke Rush, Thomas Stephens, Yan Zhou, Mark A. Delucchi, Alicia Birky, Chad Hunter, Zhenhong Lin, Shiqi Ou, Fei Xie, Camron Proctor, Steven Wiryadinata, Nawei Liu, and Madhur Boloor. Comprehensive Total Cost of Ownership Quantification for Vehicles with Different Size Classes and Powertrains. *U.S. Department of Energy, Argonne National Laboratory*, 2021. URL https://publications.anl.gov/anlpubs/2021/05/167399.pdf.

Supplementary Material

Drive Cycles in the Literature

Figure S1 shows six drive cycles commonly used for heavy-duty truck emissions modeling in the USA. The US EPA has been using the Highway fuel consumption Driving Schedule (HWFET), US06 Supplemental Federal Test Procedure and Heavy-Duty Urban Dynamometer Driving Schedule (HDUDDS). The California Air Resources Board (CARB) introduced the Heavy-Duty Diesel Truck Cruise Mode (HHDDT). The Northeast States Center for a Clean Air Future (NESCCAF) and the National Renewable Energy Laboratory (NREL) also developed their own long-haul cycles.

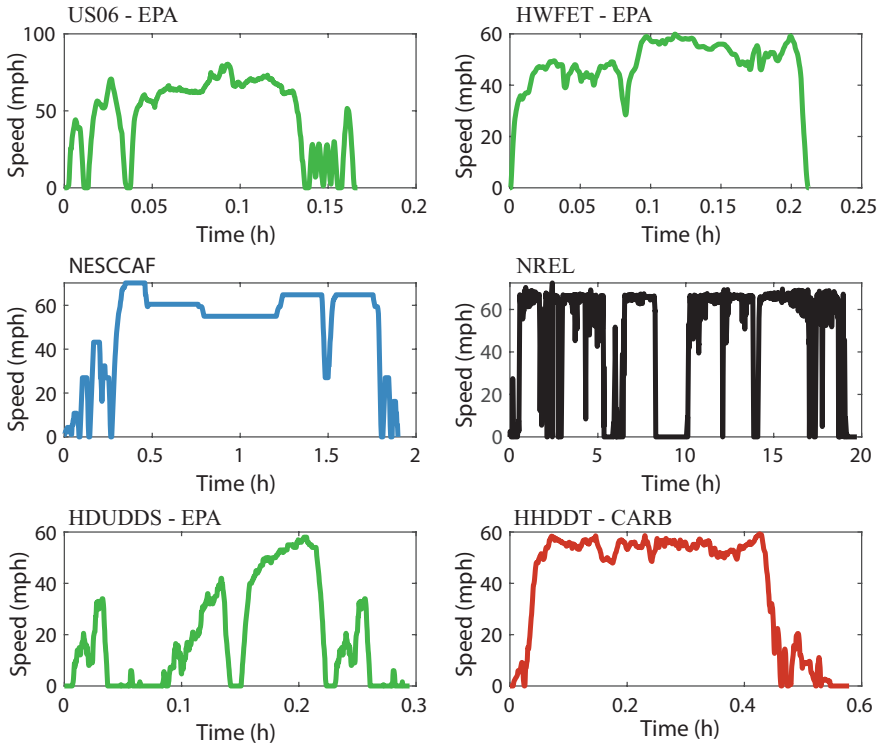

Figure S1: Standard drive cycles used for long-haul trucks: a) US06, b) HWFET, c) NESCCAF, d) NRTL, e) HDUDDS, and f) HHDDT.Source:[1, 2, 3, 4, 5]

Defining Long Haul

The vehicle miles traveled for a truck with a 10-year vehicle lifetime are given in Table S1.Figure S2 shows the total number of class 8 trucks with sleeper cabs in the VIUS 2002 dataset.

The daily range distribution for all class 8 trucks is shown in Figure S3. For class 8 trucks with a sleeper cab, the distribution is depicted in Figure S4.

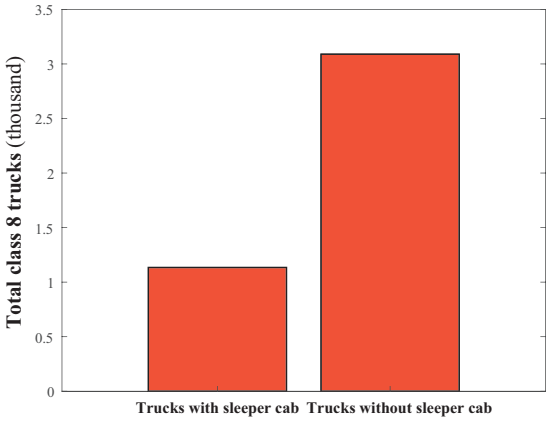

Figure S2: Class 8 trucks with sleeper cabs (defined as long-haul) according to the VIUS dataset [6]

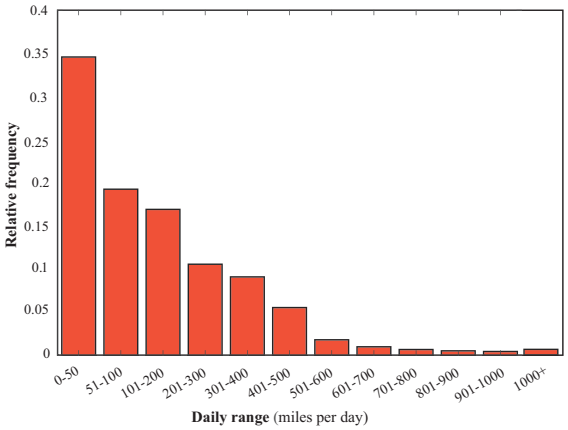

Figure S3: Daily range distribution for all class 8 trucks in VIUS dataset [6, 7]. onversion factor from years to days given by months under operation, 30.4 days in a month and 60/34 work period

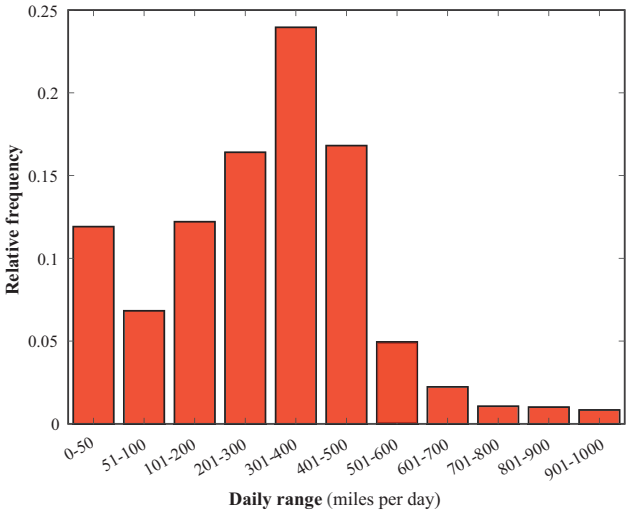

Figure S4: Daily range of class 8 trucks with sleeper cabs from the VIUS database. Conversion factor from years to days given by months under operation,30.4 days in a month, and 60/7/34 work period. [7, 6]

Table S1: Annual average vehicle miles traveled of long-haul class 8 trucks in the USA [8]

Year of vehicle life	Vehicle miles traveled
1	108,000
2	120,000
3	114,000
4	105,000
5	92,000
6	81,000
7	74,000
8	67,000
9	59,000
10	52,000

Target Feature Vector Definition

The target feature vector was defined according to the vehicle speed and absolute road grade distributions shown in Figure S5 and Figure S6. The individual shares in S5 are in 5 % increments because that is the highest resolution available for all datasets. Descriptions of the datasets used for the target feature vector can be found in Table S2. The target vector is available in Table S3.

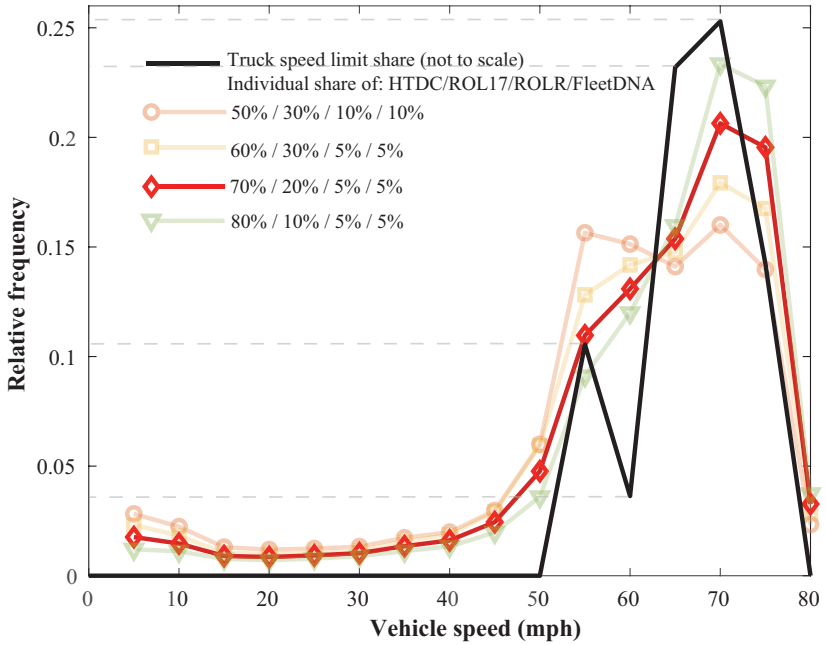

Figure S5: Vehicle speed distributions of different dataset combinations

Drive Cycle Generation

Data pre-processing: The Run on Less Regional (ROLR) raw dataset was provided under a collaboration agreement with the North American Council for Freight Efficiency (NACFE). A set of concatenated files for each truck was created for further data cleansing. This cleansing process includes the detection and correction of corrupt, coarse, or inaccurate data, which enables a more representative characteri-

Table S2: Overview of datasets considered for the target vector definition [9] [10] [11] [12]

Dataset	Description
ROL17	• 7 trucks over a period of 17 days. Over 50,107 miles of data collected • Average driving speed of 54 mph, very little time was spent at 68 mph or higher • Average mileage of 506 miles/day • Data collection with a focus on longer haul driving • Relatively good geographical coverage of the main long-haul freight routes of the US, but concentrated in the Midwest and Southeast of the US.
ROLR	• 10 trucks over a period of 18 days. Over 58,000 miles of data collected • Average driving speed of 53.21 mph, but significantly more zero-speed time and significantly higher number of stops in comparison to ROL17 • All trucks drove over 350 miles per day with an average mileage of 434 miles/day • Not a dedicated long-haul data collection. Focus on Regional-haul with more frequents stops and therefore more frequent acceleration events • Limited geographical coverage because of locally concentrated regional-haul scope.
HTDC	• 6 trucks over a period of 12 months. 637,558 miles of data collected • Average driving speed of 66.82 mph • Dedicated long-haul data collection • Very good coverage of the Southern and Eastern US, but no coverage of the West Coast of the US • Very good temporal coverage: captures seasonal variations
Filtered fleet DNA	• 12 trucks and 7247.4 miles of data collected. No information about the exact duration of the data collection period • Average driving speed of 45.57 mph • Dataset filtered to select long-haul driving, but not a dedicated long-haul data collection • Geographical coverage Heavy bias towards states on the West Coast of the US
TomTom N.V. National Road Grade Database	• 100 % coverage of US controlled access highway routes • approx. 12 million measured datapoints with an accuracy on road grade of ±0.3 % • Validated against datasets by Southwest Research Insitute and US Geological Survey • Based thereon: "Development of Road Grade Profiles Representative of US Controlled Access Highways" [13]

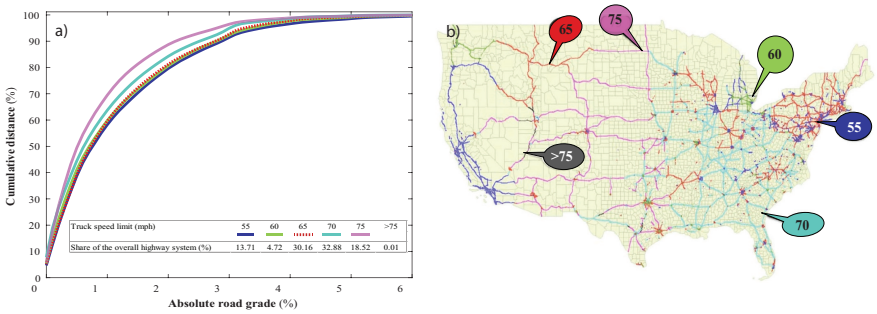

Figure S6: a) Activity-weighted, distance-based cumulative distribution of absolute road grade by truck speed limit, b) State-defined truck speed limit on US controlled access highway. Adapted from:[13]

Table S3: Target vector for long-haul drive cycle construction

Target road grade vector				**Target speed vector**	
Interval (%)	Relative frequency	Interval (%)	Relative frequency	Interval (mph)	Relative frequency
[-6; -5)	0.000962	(0; 0.1]	0.079101	(0; 5]	0.017636
[-5; -4)	0.000524	(0.1; 0.2]	0.039151	(5; 10]	0.014692
[-4; -3.5)	0.0013954	(0.2; 0.3]	0.0341882	(10; 15]	0.009007
[-3.5; -3)	0.001678	(0.3; 0.4]	0.031951	(15; 20]	0.008556
[-3; -2.6)	0.005869	(0.4; 0.5]	0.030012	(20; 25]	0.00928
[-2.6; -2.3)	0.004532	(0.5; 0.6]	0.025255	(25; 30]	0.010288
[-2.3; -2)	0.00547	(0.6; 0.7]	0.020996	(30; 35]	0.013487
[-2; -1.8)	0.007702	(0.7; 0.8]	0.018812	(35; 40]	0.01611
[-1.8; -1.6)	0.008405	(0.8; 0.9]	0.017279	(40; 45]	0.024457
[-1.6; -1.4)	0.009555	(0.9; 1]	0.016175	(45; 50]	0.047686
[-1.4; -1.2)	0.011091	(1; 1.2]	0.013247	(50; 55]	0.10966
[-1.2; -1)	0.013247	(1.2; 1.4]	0.011091	(55; 60]	0.130886
[-1; -0.9)	0.016175	(1.4; 1.6]	0.009555	(60; 65]	0.15372
[-0.9; -0.8)	0.017279	(1.6; 1.8]	0.008405	(65; 70]	0.206397
[-0.8; -0.7)	0.018812	(1.8; 2]	0.007702	(70; 75]	0.195433
[-0.7; -0.6)	0.020996	(2; 2.3]	0.00547	(75; 80]	0.032708
[-0.6; -0.5)	0.025255	(2.3; 2.6]	0.004532		
[-0.5; -0.4)	0.030012	(2.6; 3]	0.005869		
[-0.4; -0.3)	0.031951	(3; 3.5]	0.001678		
[-0.3; -0.2)	0.034188	(3.5; 4]	0.001395		
[-0.2; -0.1)	0.039151	(4; 5]	0.000524		
[-0.1; -0)	0.079101	(5; 6]	0.000962		

zation of the long-haul cycles.

1. Remove duplicates and incomplete data: duplicate vehicle speed profiles and vehicle data lacking several important signals were removed.
2. Remove unrealistic datapoints: Outliers representing the maximum possible OBD vehicle speed value of 255.99 km/h for an increment of only one second were removed from the dataset since the maximum vehicle speed in a realistic progression is 124.5 km/h. For values above 150 km/h, the datapoints were replaced by a linear interpolation of the previous and the subsequent error-free datapoints.
3. Check data quality of raw elevation signal: No extreme outliers were detected for the elevation signal, but noise. Hence, the Savitzky-Golay filter was applied to denoise the signals.

Acceleration and road grade estimation: The vehicle acceleration was calculated using the cleansed speed datapoints. The road grade (RG) was calculated from both elevation signal and vehicle speed signal. As shown in Equation S1, the road grade (%) derives from the difference in elevation (rise) divided by the difference in distance (run) between two sampling points.

$$RG(\%) = \frac{\Delta Elevation}{\Delta Distance} * 100 = tan\alpha * 100 \tag{S1}$$

Microtrip preparation: The microtrip based cycle approach was used for the construction of the drive cycle. These microtrips were prepared as follows:

1. Cutting of the ROLR data into microtrips: the datapoints with vehicle speed and acceleration of zero were used to define connecting points between consecutive microtrips. Based on these

bounded points, the microtrips were cut from the ROLR data. All other datapoints were discarded.

2. Smoothing the microtrip elevation at connecting points: the elevation values were smoothed at the connecting points to ensure that the resulting road grades were equal to zero. This leads to a more consistent sequence of microtrips and continuous road grade traces.
3. Determination of feature vector for each microtrip: the vehicle speed trace was integrated over time to obtain the total distance driven per microtrip. The average speed value was then estimated as the arithmetic mean of the vehicle speed trace. The relative frequency of each 5-mph vehicle speed interval was determined as the ratio of the total number of datapoints within a given interval to the total number of datapoints of the microtrip. Similarly, the relative frequency of the road grade intervals was calculated from the road grade trace of each microtrip.
4. Microtrips classification into long-haul and urban: the microtrips were separated into an urban pool representing the drive out of or into a metropolitan area and a long-haul pool representing the prolonged highway driving in between metropolitan areas. This distinction was made according to the criteria summarized in Table S4. All microtrips that could neither be classified as long-haul nor as urban were discarded.

Table S4: Classification criteria for long-haul and urban microtrips

Criteria	Value	Unit	Reference
Minimum highway distance	105.66	miles	This work
Minimum average driving speed	40	mph	[14]
Driving time between stops	2	hours	(J. Gregorio, personal communication, Sept 5, 2021)
Complete stops on interstate	No	-	(J. Gregorio, personal communication, Sept 5, 2021)
Minimum urban distance	15	mi	This work
Total urban distance	30	mi	This work

Microtrips random selection: After the microtrip preparation process, an algorithm for the random selection and evaluation of microtrips was programmed and applied to the data. The randomized drive cycle generation process constructs drive cycles in two segments. First, the long-haul segment is generated with randomly selected microtrips from the long-haul microtrip pool. In detail, microtrips are successively selected at random and their cumulative distance is calculated with each microtrip selection. If the sum of the current cumulative distance and the distance of the next microtrip candidate exceeds the maximum distance for the long-haul segment, the long-haul fail counter is incremented by one. The maximum long-haul segment distance is equal to the maximum total distance subtracted by the initialized urban distance. If the fail counter is greater than the initialized maximum fail counter value, the generation of the long-haul segment is terminated. It is important to consider that the described optimization for a maximum distance leads to a bias of shorter microtrips towards the end. Therefore, all microtrips of the segment are randomly reshuffled before they are concatenated. Analogous to the long-haul segment, the urban segments are generated at either end of the long-haul segment. Microtrips are also successively selected at random and then randomly added to either the beginning or the end of the already generated long-haul segment. The urban fail counter is incremented by one if adding the distance of the next candidate microtrip would exceed the maximum total distance. Microtrips from the urban pool are excluded from the process if their distance is greater than 50 % of the remaining distance until the initialized maximum. This was done after initial trial runs to increase the efficiency of the algorithm and to prevent the urban segment from consisting of only very few and long microtrips. Again, the generation of the urban segment is terminated when the maximum value of the urban fail counter is exceeded and then the generated segment is reshuffled. The urban segments are created last because the urban microtrips are significantly shorter than the long-haul microtrips. Consequently, the urban segment has a higher variability and is more adaptable to converge towards the target feature vector and towards the defined maximum distance.

Drive cycle evaluation: Through this step, each resulting drive cycle is compared to the national average driving profile. The deviation of each feature in the microtrips from the target vector is estimated and

used to calculate the absolute error of the entire drive cycle. The contribution of each microtrip to the absolute error was time-weighted. Since the complete target vector accounts for 63 features, namely, distance, average vehicle speed, 16 vehicle speed distribution intervals and 44 road grade distribution intervals, weighting factors were introduced to account for the relative importance of each feature to the error. In this work, the weighting factors for distance feature, vehicle speed and road grade were set at 0.1,0.54 and 0.36, respectively. Based on these weights, a single error value is obtained for each generated drive cycle using the Euclidian norm of the weighed deviation vector. Finally, the drive cycle with smallest error was selected, and was named as USLHC8 (i.e. US Long-Haul Class 8 drive cycle). The Kolmogorov-Smirnov test was chosen for this validation since, on the one hand, it is sensitive to differences in both shape and location of the distributions in consideration. On the other hand, it is widely used in the literature for evaluating the statistical similarity of two cumulative distributions [15, 16].

We also sampled other drive cycles generated with the algorithm for a 600-mile range. The distribution of vehicle speeds was distinguishable between individual random sampling. However, they have relatively close vehicle speeds (between 52 and 56 mph and variances between 343 and 259 mph^2, respectively), and fuel consumption around $\sim$ 7.6 and 7.2 mpg. To illustrate the capabilities of the algorithm to generate drive cycles of different lengths, we also generated drive cycles with a 300-mile range. Sampling from a few possible 300-mile drive cycles showed close fuel consumption ($\sim 7.6 - 7.4$ mpg) and average vehicle speeds between 51 and 56 mph with variance between 302 and 143 mph^2, respectively.

Truck modeling

Simulations across the USLHC8 drive cycle were limited to no more than a 1.24 mph average error. The error was defined as:

$$Absolute\ Mean\ Error = \frac{\int_0^{t_f} \sqrt{(v_{USLHC8} - v_{simulated})^2}}{t_f} \tag{S2}$$

Where v_{USLHC8} is the velocity of the USLHC8 drive cycle, $v_{simulated}$ is the velocity of vehicle being simulated, and t_f is the total time of the drive cycle.

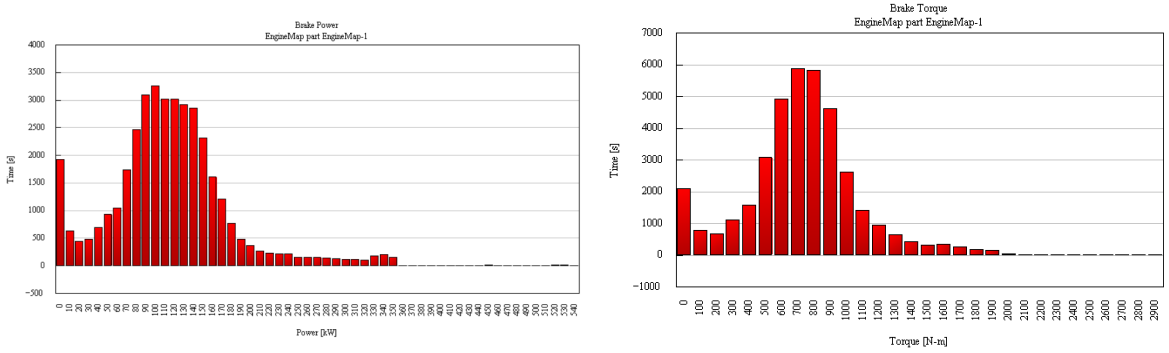

Figure S7: Output space for engine sizing

Shifting Optimization

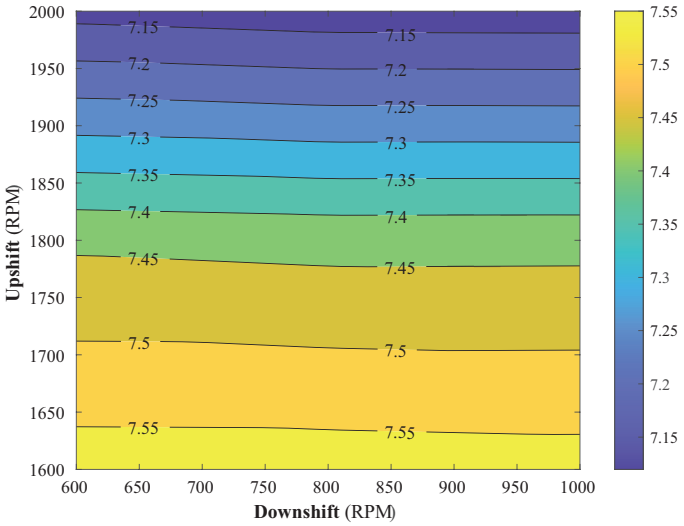

Figure S8: Effect of gear shift strategies on fuel consumption

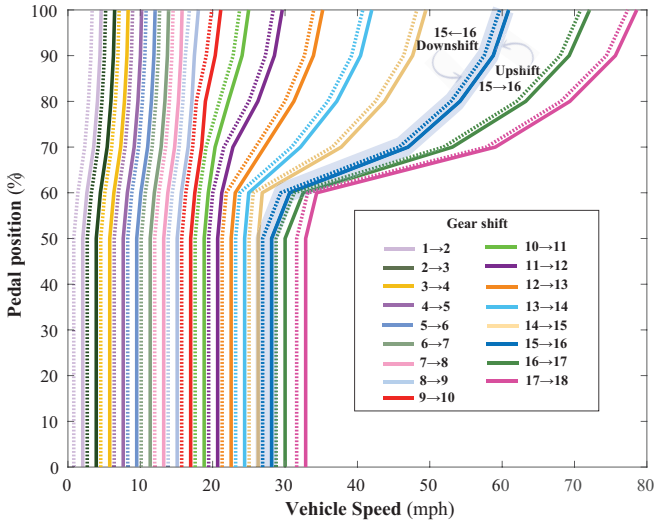

Figure S9: Shift schedule generation. Downshifting in dotted lines

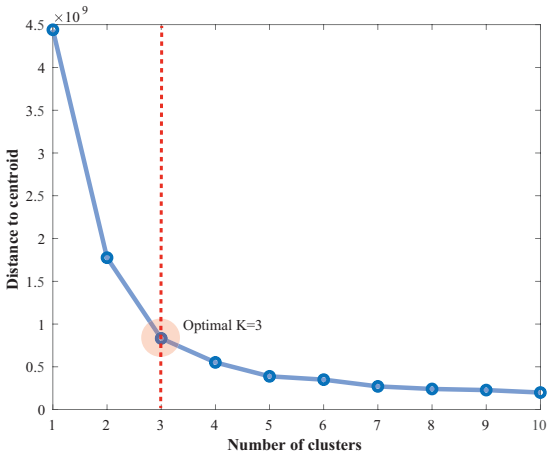

Figure S10: Optimal number of clusters using elbow method

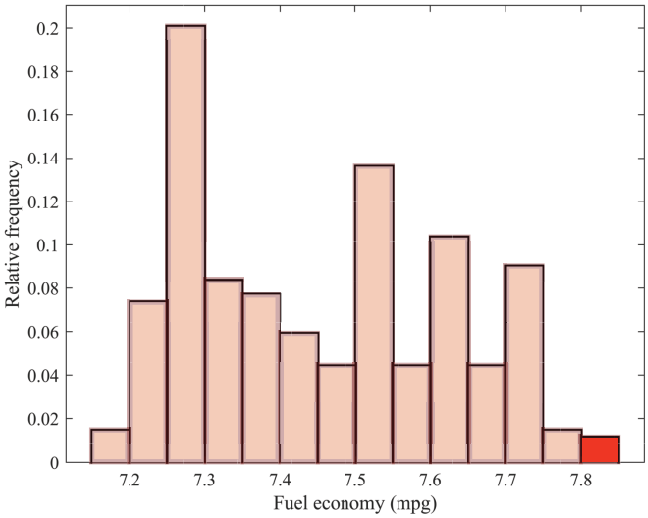

Figure S11: Output space of fuel economies in case sweep

Table S5: Optimization results for sweep case

Variable	Minimum	Maximum	Optimized
Final drive ratio	2.9	3.9	3.04
16th gear	0.8	1.1	0.82
17th gear	0.65	0.9	0.75
18th gear	0.55	0.8	0.71

Total Cost of Ownership Model

Discount rate: The discount factor is calculated according to equation

$$DF = \left(\frac{1}{1+DR}\right)^{yr} \tag{S3}$$

Where DF is the discount factor, DR is the discount rate, and yr is the year

Operating cost: The operating cost considers labor, maintenance & repair, tolls, permits & licenses, fuel and insurance. The cost of these components per mile travelled was translated to total operating costs using the VMT per year and the discount factor as given in Equation S5.

$$Operating\,Cost = \$_{Labor} + \$_{M\&R} + \$_{Tolls} + \$_{Permits\&Licenses} + \$_{Fuel} + \$_{Insurance} \tag{S4}$$

$$Operating\,Cost_i = \sum_{yr=1}^{10}\left(\frac{\$}{mi} \times VMT_{yr} \times DF_{yr}\right) \tag{S5}$$

Capital cost: The capital cost considers engine, aftertreatment, transmission, waste heat recovery, fuel tank, and glider manufacturing costs. The total capital cost is given by Equation S6.

$$Capital\,Cost = \$_{Engine} + \$_{aftertreatment} + \$_{Transmission} + \$_{WHR} + \$_{Tank} + \$_{Glider} \tag{S6}$$

The manufacturing costs for the engine and the aftertreatment system are depicted in Figure S12

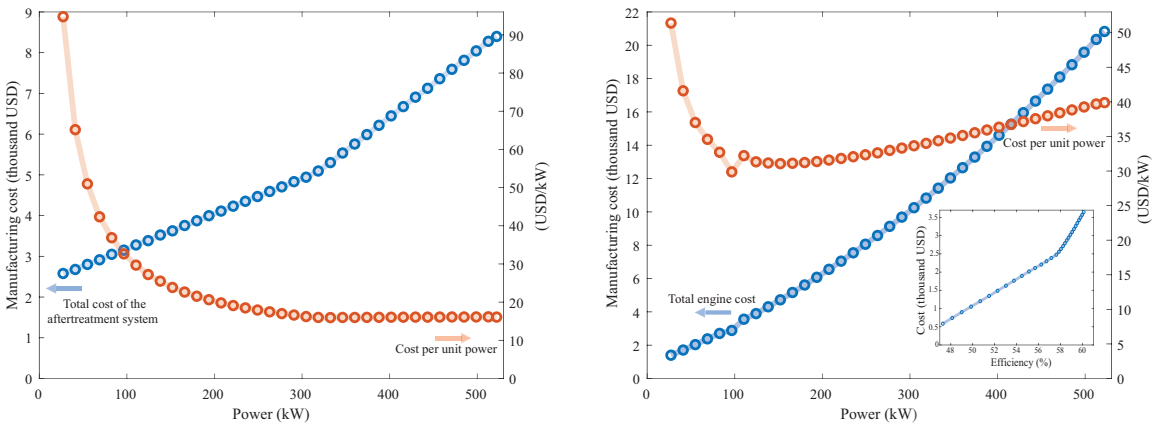

(a) After-treatment

(b) Engine

Figure S12: Manufacturing cost as function of power demand

References

[1] U.S. Environmental Protection Agency. Vehicle and fuel emissions testing: Dynamometer drive schedules, 2021. URL https://www.epa.gov/vehicle-and-fuel-emissions-testing/dynamometer-drive-schedules.

[2] Dieselnet. Heavy heavy-duty diesel truck (hhddt) schedule, 2007. URL https://dieselnet.com/standards/cycles/hhddt.php.
[3] Yang Wenli. Heavy duty diesel vehicle exhaust pm speciation profiles, 2014. URL https://ww2.arb.ca.gov/speciation-profiles-used-carb-modeling.
[4] NESCCAF Northeast States Center for a Clean Air Future; ICCT International Council on Clean. Heavy-duty long haul combination truck fuel consumption and co 2 emissions, 2009.
[5] Chen Zhang, Andrew Kotz, Kenneth Kelly, and Luke Rippelmeyer. Development of heavy-duty vehicle representative driving cycles via decision tree regression. *Transportation Research Part D: Transport and Environment*, 95:102843, 2021. ISSN 1361-9209. doi: https://doi.org/10.1016/j.trd.2021.102843. URL https://www.sciencedirect.com/science/article/pii/S1361920921001462.
[6] Thomas Zabelsky, John Miller, Ruth Detlefsen, Bernard Fitzpatrick, Dennis Stoudt, Barry Sessamen, and Robert Brown. 2002 economic census: Vehicle inventory and use survey, 12 2004. URL https://www2.census.gov/library/publications/economic-census/2002/vehicle-inventory-and-use-survey/ec02tv-us.pdf.
[7] Federal Motor Carrier Safety Administration. Summary of hours of service regulations, 3 2022. URL https://www.fmcsa.dot.gov/regulations/hours-service/summary-hours-service-regulations.
[8] Andrew Burnham, David Gohlke, Luke Rush, Thomas Stephens, Yan Zhou, Mark A. Delucchi, Alicia Birky, Chad Hunter, Zhenhong Lin, Shiqi Ou, Fei Xie, Camron Proctor, Steven Wiryadinata, Nawei Liu, and Madhur Boloor. Comprehensive Total Cost of Ownership Quantification for Vehicles with Different Size Classes and Powertrains. *U.S. Department of Energy, Argonne National Laboratory*, 2021. URL https://publications.anl.gov/anlpubs/2021/05/167399.pdf.
[9] Yunsu Park, Mike Roeth, Denise Rondini, David Schaller, and Bianca Wachtel. Run on less report, 2018.
[10] Rick Mihelic, David Schaller, Yunsu Park, Kevin Otto, Mike Roeth, and Denise Rondini. Run on less regional report, 2020.
[11] Gary Capps, Oscar Franzese, Bill Knee, Mary Beth Lascurain, and Pedro Otaduy. Class-8 Heavy Truck Duty Cycle (Report No. ORNL/TM-2008/122), 2008. URL http://www.osti.gov/bridge.
[12] K Walkowicz, K Kelly, A Duran, and E Burton. Fleet dna project data, 2019.
[13] Eric Wood, Adam Duran, and Kenneth Kelly. Epa ghg certification of medium- and heavy-duty vehicles: Development of road grade profiles representative of us controlled access highways. *SAE International Journal of Fuels and Lubricants*, 9, 2016. ISSN 19463960. doi: 10.4271/2016-01-8017.
[14] Kanok Boriboonsomsin, Kent Johnson, George Scora, Daniel Sandez, Alexander Vu, Tom Durbin, and Yu Jiang. Collection of activity data from on-road heavy-duty diesel vehicles collection of activity data from on-road heavy-duty diesel vehicles final report, 2017.
[15] MIT. Open courseware. section 13: Kolmogorov-smirnov test, 2006.
[16] MathWorks. Matlab documentation: Two-sample kolmogorov-smirnov test, 2021.